Higher Angiotensin I Converting Enzyme 2 (ACE2) levels in the brain of individuals with Alzheimer's disease.

Reveret Louise[1,2] (louise.reveret.1@ulaval.ca),

Leclerc Manon[1,2] (manon.leclerc.4@ulaval.ca),

Emond Vincent[2] (vincent.emond@crchudequebec.ulaval.ca),

Loiselle Andréanne[2] (andreanne.loiselle@crchudequebec.ulaval.ca),

Bourassa Philippe[1,2] (philippe.bourassa.4@gmail.com),

Tremblay Cyntia[2] (cyntia.tremblay@crchudequebec.ulaval.ca),

Bennett David A[4] (David_A_Bennett@rush.edu),

Hébert Sébastien[2,3] (Sebastien.Hebert@crchudequebec.ulaval.ca),

and Calon Frédéric[1,2] (Frederic.calon@pha.ulaval.ca).

Author affiliations:

1. Faculty of pharmacy, Laval University, Quebec, QC, Canada

2. CHU de Quebec Research Center, Quebec, QC, Canada

3. Faculty of medicine, Laval University, Quebec, QC, Canada

4. Rush Alzheimer's Disease Center, Rush University Medical Center, Chicago, IL, USA

Corresponding author: Frédéric Calon

Centre de Recherche du CHUL (CHUQ)

2705, Boulevard Laurier, Room T2-05

Québec, QC, G1V 4G2, Canada

Frederic.calon@pha.ulaval.ca

Abstract

The severe acute respiratory syndrome coronavirus 2 (SARS-CoV-2) is a major cause of death in the elderly. Cognitive decline due to Alzheimer's disease (AD) is frequent in the geriatric population disproportionately affected by the COVID-19 pandemic. Interestingly, central nervous system (CNS) manifestations have been reported in SARS-CoV-2-infected patients. In this study, we investigated the levels of Angiotensin I Converting Enzyme 2 (ACE2), the main entry receptor of SARS-COV-2 in cells, in *postmortem* parietal cortex samples from two independent AD cohorts, totalling 142 persons. Higher concentrations of ACE2 protein and mRNA were found in individuals with a neuropathological diagnosis of AD compared to age-matched healthy control subjects. Brain levels of soluble ACE2 were inversely associated with cognitive scores ($p = 0.02$), markers of pericytes (PDGFRβ, $p=0.02$ and ANPEP, $p = 0.007$) and caveolin1 ($p = 0.03$), but positively correlated with soluble amyloid-β peptides (Aβ) concentrations ($p = 0.01$) and insoluble phospho-tau (S396/404, $p = 0.002$). No significant differences in ACE2 were observed in the 3xTgAD mouse model of tau and Aβ neuropathology. Results from immunofluorescence and Western blots showed that ACE2 protein is mainly localized in neurons in the human brain but predominantly in microvessels in the mouse brain. The present data show that an AD diagnosis is associated with

higher levels of soluble ACE2 in the human brain, which might contribute to a higher risk of CNS SARS-CoV-2 infection.

Key Words: ACE2; Alzheimer's disease; Cognitive dysfunction.

Introduction.

SARS-CoV-2 (Severe Acute Respiratory Syndrome CoronaVirus 2), the cause of Coronavirus disease 2019 (COVID-19), remains a significant public health concern. Epidemiological studies have shown that fatality rates increase with age, particularly after 65 years of age [40]. In terms of death and other clinical complications, people with dementia are disproportionately impacted by COVID-19 [14, 44, 62, 66, 86]. Whether this is due to age *per se* or other factors associated with cognitive decline is currently unknown.

Although the SARS-CoV-2 virus mainly infects lower respiratory and nasopharyngeal tracts, causing respiratory failure, CNS manifestations have also been described in more than one third of hospitalized patients, especially those with severe condition [14, 46, 49, 52, 61, 85, 86]. Non-specific neurological symptoms like headache and dizziness are also commonly observed in different cohorts [33, 49] but other neurological complications reported include ischaemic stroke [8], encephalopathy [34], meningo-encephalitis [34], demyelination [87], infarcts and microhaemorrhages [26, 48].

An association between COVID-19 infection and cognitive decline due to Alzheimer's disease (AD) or other causes is emerging. Risk factors for COVID-19 complications are often the same as those for dementia - age, obesity, cardiovascular disease, hypertension, and diabetes mellitus [44, 63, 79]. Notably, dementia *per se* is a strong predictor of COVID-19 mortality [50]. Using de-

identified population-level electronic health records (EHR) from over 60 million individuals, a retrospective study showed that patients with dementia and COVID-19 had significantly worse outcomes (6-month hospitalization risk and mortality risk) than patients with dementia and no COVID-19 or patients with COVID-19 but no dementia [79]. This association remained significant after adjusting for age, sex and known COVID-19 risk factors (including, for example type 2 diabetes, cardiovascular diseases, pulmonary diseases, asthma and others). Concerns have also been raised that COVID-19 increases the risk of developing cognitive impairments, possibly secondary to cerebral ischemia in brain areas linked to cognition [3, 21, 39, 54].

Angiotensin I Converting Enzyme 2 (ACE2) is a membrane carboxypeptidase considered the main site of entry of SARS-CoV-2 into cells [38, 45, 64]. ACE2 is highly expressed in the lung, consistent with respiratory dysfunction being the first clinical consequence of the infection [15, 28]. Interestingly, ACE2 is expressed in other tissues such as the kidney, intestine, liver, testis and brain [36, 67]. The distribution of ACE2 in the brain is controversial, and original reports failed to identify the protein in the human CNS [19, 73]. Still, low levels of ACE2 mRNA were detected in the human brain using quantitative real-time RT-PCR [30]. Cerebral immunostaining was reported in endothelial and arterial smooth muscle cells [29], as well as in neurons [20]. More recently, single-cell RNA sequencing data have brought new insights on the cellular distribution of ACE2 transcripts in the brain vasculature. According to the Betsholtz mouse database, the expression of ACE2 is very high in microvascular mural cells (such as pericytes and venous vascular smooth muscle cells), but not in endothelial cells [32, 57, 77]. However, other databases report ACE2 mRNA expression in endothelial cells of mice [15, 88, 89]. So far, the available data suggest that the expression of ACE2 is lower in both endothelial cells and pericytes in the human brain compared to the mouse brain, albeit with important interregional variability [15, 31, 51, 84, 85]. In

previous outbreaks of SARS-CoV, which also use ACE2 as an entry point, the virus was detected in the brains of infected patients but reported almost exclusively in neurons [18, 29, 58, 71]. Based on the above evidence, ACE2 expression in cells forming the neurovascular unit could provide a means by which SARS-CoV-2 enters the CNS.

Here, to investigate whether ACE2 levels in the brain could be associated with cognitive dysfunction, we compared mRNA and protein levels of ACE2 in *postmortem* brain samples from individuals of two different cohorts, including subjects diagnosed with AD. In the first cohort from the Religious Order Study (n=60), ACE2 protein levels were evaluated according to (i) the clinical diagnosis of no cognitive impairment (NCI), mild cognitive impairment (MCI), or AD, (ii) the neuropathological diagnosis of AD (ABC scoring) and the *antemortem* assessment of cognitive function. Associations between ACE2 and neurovascular markers were also examined. In the second cohort from other US sources (n=82), the relationships between brain ACE2 and mRNA concentrations were investigated in individuals with a Braak-based neuropathological AD diagnosis. Finally, we compared the cellular localization of ACE2 between human and mouse brains and assessed ACE2 levels in a triple transgenic mouse model of AD neuropathology, the 3xTg-AD mouse.

Materials and methods

Human samples

Cohort #1

Gray matter samples from the Brodmann area 7 (BA7) corresponding to the posterior parietal cortex were obtained from participants in the Religious Orders Study *(Rush Alzheimer's Disease Center)*, an extensive longitudinal clinical and pathological study of aging and dementia [5, 6]. Each participant enrolled without known dementia and underwent annual structured clinical evaluations until death. A total of 21 cognitive performance tests were performed for each subject. At the time of death, a neurologist, blinded to all *postmortem* data, reviewed clinical data and rendered a summary diagnostic opinion regarding the clinical diagnosis proximate to death. Participants thus received a clinical diagnosis of NCI (n = 20) or MCI (n = 20) or AD (n = 20), as previously described [5-7]. The neuropathological assessment for the subjects included in the present study was performed using the ABC scoring method found in the revised National Institute of Aging – Alzheimer's Association (NIA-AA) guidelines for the neuropathological diagnosis of AD [56]. Three different neuropathological parameters were evaluated for each subject: (A) the Thal score assessing phases of Aβ plaque accumulation [72] , (B) the Braak score assessing neurofibrillary tangle pathology [13] and (C) the CERAD score assessing neuritic plaque pathology [55]. These scores were then combined to obtain an ABC score, reported as AX, BX and CX with X ranging from 0 to 3 for each parameter [56]. To determine a dichotomic neuropathological diagnosis in accordance with the revised NIA-AA guidelines [56], participants with intermediate or high levels of AD neuropathological markers were classified as AD, whereas participants with no or a low level of AD neuropathological changes were classified as Controls. Relevant data from the ROS samples used here are summarized in Table 1.

Cohort #2

Gray matter samples from the parietal cortex were obtained from 3 different institutions in the United States: 1- *Harvard Brain Tissue Resource Center*, Boston, Massachussetts, 2- *Brain Endowment Bank*, Miami, Florida. 3- *Human Brain and Spinal Fluid Resource Center*, Los Angeles, California [23]. All 82 parietal cortex samples were from the Brodmann area 39 (BA39), corresponding to the inferior region of the parietal cortex. Neuropathological diagnoses were based on Braak scores that were available for all cases. Braak scores of I or II were classified as Controls while Braak scores of III, IV, V and VI were considered as AD (Table 1).

Immunostaining

To demonstrate ACE2 localization in *postmortem* human brain tissue, we tested a number of commercially available antibodies using a wide range of immunostaining protocols. Immunostaining was performed on formalin-fixed, paraffin-embedded (FFPE) tissue sections (6 µm) of human parietal cortex, on fresh-frozen (FF) tissue sections (12 µm) from human and mouse hippocampus, as well as on human and murine isolated brain microvessels (see below). Briefly, FFPE sections were deparaffinized in CitriSolv hybrid and rehydrated with decreasing concentrations of ethanol in water. Antigen retrieval was then performed by boiling slides in Tris buffer (10 mM, pH 9.0) with 1 mM EDTA and 0.05% (v/v) Tween-20 in a microwave for 15 minutes and letting them cool for 30 minutes at room temperature. Sections were quenched with 50 mM NH_4Cl, digested with trypsin 0.1% (w/v, Sigma-Aldrich) at 37°C for 15 min, and incubated in Tris-buffered saline (TBS) with 0.3 M glycine for 15 minutes. Sections were then blocked sequentially with Bloxall, avidin/biotin blocking kit (Vector Laboratories, CA) and Superblock (Thermo) with 0.2% Triton-X100, and used for immunohistochemistry. FF sections and brain microvascular fractions were kept at -80°C until use, then vacuum-dried at 4°C and fixed in 4%

(w/v) paraformaldehyde (pH 7.4) for 20 min at room temperature. All sections were then blocked and permeabilized for 1h with Superblock containing 0.2% (v/v) Triton X-100. Incubation with primary antibodies (various rabbit anti-ACE2, mouse anti-NeuN MAB377, goat anti-collagen IV AB789) was performed overnight at 4°C in Superblock with 0.05% Tween-20. For immunohistochemistry, after multiple washing in PBS, sections were incubated with biotinylated secondary antibodies (Jackson Immunoresearch) and then with streptavidin-HRP (ABC Elite kit). ACE2 localization was revealed using the ImmPACT AMEC red substrate and nuclei were counterstained with Mayer's hematoxylin. For immunofluorescence, after washes, secondary antibodies (conjugated to Alexa Fluor 555, 647 and 750, which use channels with less autofluorescence) were added to sections for 1h. Slides were then sequentially incubated with 4′,6-diamidino-2-phenylindole (DAPI) and TrueBlack Plus (Biotium, CA). Photomicrographs were recorded with a Cytation 5 or EVOS fl Auto Imaging System (Thermo Fisher).

Protein fractionation from human parietal cortex homogenates

Each inferior parietal cortex sample (~100 mg) from the Cohort #1 was sequentially sonicated and centrifuged to generate two protein fractions: a Tris-buffered saline (TBS)-soluble fraction containing soluble intracellular, nuclear and extracellular proteins and a detergent-soluble protein fraction containing membrane-bound proteins extracted with a mix of detergents (0.5% Sodium dodecyl sulfate (SDS), 0.5% deoxycholate, 1% Triton), as previously reported [74, 75]. For samples of the Cohort #2, frozen extracts from the parietal cortex were ground into a fine powder on dry ice with a mortar and pestle. Approximatively 50 mg of this fine powder was used for total protein extraction. Then, a lysis buffer (50 mM Tris-HCL to pH 7.4, 150 mM NaCl, 1% triton and 0.5% sodium deoxycholate) containing protease (complete 25 X and Pepstatin A) and phosphatase inhibitors (sodium fluoride and sodium vanadate) was added in the proportion of 4 times the sample

weight (400 µL for 50 mg). The sample solution was homogenized on ice by sonication using a Sonic Dismembrator (Fisher, Pittsburgh, PA) with two 10-second pulses and a 30-second stop between steps. Samples were centrifuged 20 minutes at 10,000 g at 4 °C. Protein contents of supernatants were quantified using a bicinchoninic acid assay (Thermofisher cat: P123227). Protein homogenates in Laemmli were prepared as described below.

Isolation of human brain microvessels

The method used to generate microvessel-enriched extracts from frozen human parietal cortex samples has been described in our previous publications [10-12]. Briefly, this method consists of a series of centrifugation steps, including one density gradient centrifugation with dextran, after which the tissue is filtered through a 20-µm nylon filter. Two fractions were generated: one enriched in cerebral microvessels (isolated microvessel-enriched fraction) and the other consisting of microvessel-depleted parenchymal cell populations. Cerebral fractions enriched and depleted in endothelial cells were evaluated using immunoblotting of vascular and neuronal markers, as shown previously [11]. Isolation of brain microvessels was performed on human samples of Cohort #1 (final n = 57) and the fractions were used for immunostaining and Western blot analysis.

RNA extraction and RT-qPCR analysis

As mentioned above, powderized parietal cortex tissues of Cohort #2 were kept at -80°C. Approximately 100 mg of this fine powder was used for total RNA extraction with TRIzol (Ambion). Unless otherwise noted, all steps were performed on ice or at 4°C. Samples were homogenized by sonication with a Sonic Dismembrator (Fisher, Pittsburgh, PA) with 4-sec pulses in 500 µL of TRIzol. Chloroform (100 µL) was added to the solution, mixed and incubated for 2 minutes before centrifugation at 12,000 g for 15 minutes. Supernatants were kept, 250 µL of

isopropanol were added followed by a 10-min incubation at -80°C and a 10-min centrifugation, at 12,000 g. The pellet was resuspended in 500 µL of ethanol 75 % and centrifuged 5 minutes at 7500 g. The dried pellet was resuspended in 80 µL RNAse-free water and incubated 10 minutes at 57 °C. The RNA concentration was measured with an Infinite F200 (Tecan). The reverse transcription (RT) was performed with 1 µg of RNA. As a first step, genomic DNA was removed following the AccuRT Genomic DNA removal protocol (Applied Biological Materials, ABM, Vancouver, Canada). Then the RT master mix (ABM) was added to RNA samples and incubated (10 min at 25°C, 50 min at 42°C and 5 min at 85°C) as per the manufacturer's protocol. All qPCR experiments were performed on the LightCycler 480 (Roche) with the BrightGreen mix (ABM) and primers at 10 µM. After enzyme activation for 10 min at 95°C, 50 cycles were performed (15 sec at 95°C and 1 min at 60°C), followed by 1 sec at 95°C and 1 min at 45°C. Reference gene GAPDH (primers Forward: TCTCCTCTGACTTCAACAGCGAC and Reverse :CCCTGTTGCTGTAGCCAAATTC) was used to normalize the mRNA expression. The relative amounts of each transcript were calculated using the comparative Ct (2-ΔΔCt) method. For *Ace2* qPCR (primers Forward: GTGCACAAAGGTGACAATGG and Reverse: GGCTGCAGAAAGTGACATGA), 12 controls and 19 AD individuals were used. We used a cut-off of $\geq$ 35 cycles for these samples.

Isolation of murine brain microvessels and protein fractionation

Four (4) or six (6)-, 12- and 18-month-old 3xTg-AD (APPswe, PS1M146V, tauP301L) mice produced at our animal facility were used in equal numbers of males and females in each group. These mice show progressive accumulation of Aβ plaques and neurofibrillary tangles which are detectable at 12 months and are widespread after 18 months [9, 16]. Mice from our colony were fed a standard chow (Teklad 2018, Harlan Laboratories, Canada) from breeding to 5 months of

age. For microvessels extraction, mice were then fed a control diet (CD; 20%kcal from fat) or a high-fat diet (HFD; 60%kcal from fat) from 6 to 18 months of age, in order to worsen neuropathology, memory performance and also induce metabolic impairments [4, 41, 68, 76], which are associated with a higher risk of developing severe SARS-CoV-2 infections [1, 40].

The protein extraction method results in a TBS-soluble fraction (intracellular and extracellular fraction), a detergent-soluble fraction (membrane fraction) as previously described [70].

Brain microvessels from 3xTg-AD mice were generated with a protocol similar to the one used for frozen human brain samples, as reported previously [10-12] (see Supplementary material). All experiments were performed in accordance with the Canadian Council on Animal Care and were approved by the Institutional Committee at the Centre Hospitalier de l'Université Laval (CHUL).

Western blot analysis

Protein homogenates from human parietal cortex and murine whole brain extracts were added to Laemmli's loading buffer and heated 10 min at 70°C. TBS- and detergent-soluble fractions from homogenates of human parietal cortex were also added to Laemmli's loading buffer and heated 5 min at 95°C. Equal amounts of proteins per sample (8 µg for both human and murine brain microvessel extracts and 12 µg for protein homogenates of human parietal cortex, 15 µg for protein homogenates of mouse brain) were resolved by sodium dodecyl sulphate-polyacrylamide gel electrophoresis (SDS-PAGE). All samples, loaded in a random order, were run on the same immunoblot experiment for quantification. Proteins were electroblotted on PVDF membranes, which were then blocked during 1h with a PBS solution containing 5% non-fat dry milk, 0.5% BSA and 0.1% Tween-20. Membranes were then incubated overnight at 4°C with primary antibodies (rabbit anti-ACE2, #ab108252, 1:1000, rabbit anti-TMPRSS2 #ab109131, 1:1000).

Membranes were then washed three times with PBS containing 0.1% Tween-20 and incubated during 1h at room temperature with the secondary antibody (goat/donkey anti-rabbit HRP Jackson ImmunoResearch Laboratories, West Grove, PA; 1:60,000 or 1:10,000 in PBS containing 0.1% Tween-20 and 1% BSA). Densitometric analysis was performed using ImageLab (Bio-Rad). Uncropped gels of human samples immunoblot assays are shown in the Supplementary Material (Figure S5 and Figure S6).

Data and statistical analysis

An unpaired Student's t-test was performed when only two groups were compared, with a Welch correction when variances were not equal. If the data distribution of either one or both groups failed to pass the normality tests (Shapiro-Wilk test or Kolmogorov-Smirov test), groups were compared using a non-parametric Mann-Whitney test. When more than two groups were compared, parametric one-way ANOVA followed by Tukey's multiple comparison tests or two-way ANOVA were used. If criteria for variance (Bartlett's) or normality were not met, non-parametric Kruskal-Wallis ANOVA followed by Dunn's multiple comparison tests were used. If needed, data were log transformed to normalize distributions. For all data, statistical significance was set at $P < 0.05$. Individual data were excluded for technical reasons or if determined as an outlier using the ROUT (1%) method in GraphPad Prism. Statistical analysis was done by Pearson correlation to analyze the correlation between ACE2, *antemortem* evaluation and different proteins. All statistical analyses were performed with Prism 9 (GraphPad, San Diego, CA, USA) or JMP (version 16; SAS Institute Inc., Cary, IL) software.

Results

Association between ACE2 in the parietal cortex, the neuropathological diagnosis of AD and cognitive scores.

Table 1 summarizes the clinical and biochemical data from Cohorts #1 (Religious Order Study, ROS) and #2 (Other US sources). ACE2 proteins from parietal cortex samples of each subject were fractionated into TBS-soluble (cytosolic, extracellular, nuclear and secreted proteins), detergent-soluble (membrane-bound proteins) and microvessel-enriched fractions (vascular proteins). Representative Western immunoblots of ACE2 and analyses are shown in Figure 1 for Cohort #1 and Figure 2 for Cohort #2. A band migrating at approximately 100 kDa, corresponding to full-length ACE2, was observed in each fraction (Figure 1A,E,I, Figure 2A).

We first evaluated whether ACE2 protein levels in extracts from the parietal cortex from 60 individuals from the Cohort #1, ROS. When the subjects were classified according to the neuropathological ABC diagnosis, higher levels of ACE2 protein were found in TBS-soluble fractions from AD subjects compared to non-AD participants ($p = 0.0087$) (Figure 1C). When the subjects were classified according to the clinical diagnosis, only a non-significant trend towards higher ACE2 concentrations was observed in the TBS-soluble fraction, using a non-parametric Kruskal-Wallis ANOVA ($p = 0.1471$) (Figure 1B). However, the difference between AD and Controls was statistically significant when this comparison was performed only in individuals with parenchymal cerebral amyloid angiopathy ($p = 0.0022$) (pCAA; Figure S1). On the other hand, ACE2 levels assessed in the detergent-soluble fraction, enriched for membrane-associated proteins, remained similar between groups (Figure 1E-G). We next measured ACE2 protein levels in microvessel extracts. Given the high interindividual variability, only a non-significant trend

289 towards increased ACE2 protein levels was observed in individuals with an AD clinical diagnosis
290 ($p = 0.1712$) (Figure 1J, -K).

291 Interestingly, the levels of ACE2 found in TBS-soluble and microvessel-enriched fractions were
292 inversely associated with *antemortem* global cognitive scores (Figure 1D, L and Figure 3). This
293 association remained significant after adjustment for age at death and sex.

294 To corroborate these results, we performed Western immunoblots on a second series of human
295 brain samples from the Cohort #2 [23] (Figure 2A). Consistently, higher levels of ACE2 protein
296 were detected in individuals with a neuropathological diagnosis of AD (Figure 2B). In addition,
297 *Ace2* mRNA levels were significantly higher in individuals with a Braak-based diagnosis of AD
298 compared to Controls (Figure 2B), suggesting a regulation at the transcriptional level. No
299 difference was observed in the levels of transmembrane protease serine type 2 (TMRPSS2) (Figure
300 S2), a protein that plays a key role in SARS-CoV-2 infection by activating the spike protein,
301 facilitating entry into target cells using ACE2 [38].

302 **TBS-soluble ACE2 is positively associated with clinical, neuropathological, and vascular**
303 **markers of AD, while detergent-soluble ACE2 displays opposite trends**

304 Hierarchical clustering of correlation coefficients (strength of association) was performed to
305 identify variables associated with differences in ACE2 in Cohort #1. Although the leading risk
306 factor for AD is age, no significant correlation was found between ACE2 levels in all fractions
307 tested and the ages of death (Figure 3, Figure S3), which were equivalent between groups (Table
308 1). These observations suggest that the greater soluble ACE2 in individuals with AD in the ROS
309 cohort was not driven by age. However, the age interval (74-98 years) was too small to detect an
310 effect of aging *per se* on cerebral ACE2. Beside the inverse association with global *antemortem*

cognitive scores of participants (r^2 = -0.09, P < 0.05, Figure 1D and Figure 3), higher *postmortem* TBS-soluble concentrations of ACE2 were also significantly correlated with failing episodic memory, a domain predominantly affected in AD (Figure 3).

Associations were then examined with neuropathological markers of AD, previously assessed in the parietal cortex from the sample series (Figure 3). TBS-Soluble ACE2 levels were positively associated with markers that are greater in AD like diffuse plaque counts, soluble Aβ levels and insoluble phospho-tau (pS396/404 epitope) (Figure 3). In contrast, levels of detergent-soluble ACE2 were negatively associated with the insoluble phosphorylated form of TDP-43 (which is higher in AD [12]) but positively with soluble phospho-TDP-43 C-terminal fragment migrating at approximately ~35 kDa (which is lower in AD [12]) and soluble tau (Figure 3). Similarly, neurovascular proteins such as platelet-derived growth factor receptor β (PDGRFRβ), ABCB1 and Caveolin1 correlated positively with membrane-bound ACE2 but inversely with TBS-soluble and vascular forms of ACE2, which in turn correlate with ß-secretase 1 (BACE1) and Advanced glycosylation end product-specific receptor (RAGE), proteins involved in the formation and accumulation of Aβ (Figure 3).

Single-cell RNA sequencing data in the mouse and human brain show that ACE2 mRNA expression is enriched in pericytes [31, 57], and PDGFRβ, a pericyte marker, is reduced in AD [12, 53]. Here, we found that microvascular PDGFRβ and Aminopeptidase N (ANPEP) levels were negatively correlated with TBS-soluble ACE2 levels but were positively associated with detergent-soluble ACE2 levels (Figure 3, Figure S3), suggesting a possible release of ACE2 from membranes linked with pericyte-related dysfunctions at the blood-brain barrier (BBB).

Together, these results suggest that the elevation of ACE2 in TBS-soluble and, to a lesser extent, in microvessel fractions are associated with more advanced Aβ and tau pathologies and with a

pattern of changes in vascular proteins consistent with AD progression. By contrast, membrane-bound ACE2 exhibited opposite trends and was strongly associated with reduced TDP-43 proteinopathy and consolidated BBB markers.

ACE2 is observed in human and murine neurons and cerebral vessels

Localizing ACE2 within the neurovascular unit at the interface between the blood and the brain provides basic information about SARS-CoV-2 penetration into the CNS. Therefore, we sought to determine whether ACE2 protein was enriched in brain microvessel extracts compared to post-vascular parenchymal fractions and unfractionated homogenates from human (parietal cortex) and mouse (whole brain) samples (Figure 4). We found a strong enrichment of ACE2 in murine microvessels, along with endothelial (Claudin5) and pericyte (PDGFRβ) markers (Figure 4F). However, in human brain samples, ACE2 protein levels were more comparable between microvessel and parenchymal fractions, the latter being enriched in the neuronal marker (synaptophysin) (Figure 4A). Thus, these Western blot results suggest that the localization of ACE2 in the brain differs between both species, with a cerebrovascular predominance in the mouse not observed in humans.

To confirm the cellular localization of ACE2, immunostaining was also performed on fractionated brain homogenates (Figure 4B-E, G, H). A moderate immunofluorescent signal was detected inside microvessels isolated from human brains (collagen IV-positive, Figure 4B, C) and NeuN-positive neurons (Figure 4C, E). By contrast in the mouse, ACE2 immunosignal was intense in microvessels and colocalized well with collagen IV (Figure 4G, H). To validate immunostaining in human tissue sections, nine anti-ACE2 antibodies were used in human testis samples where ACE2 is highly expressed in Leydig and Sertoli cells (Figure S4). All antibodies showed a clear signal in this tissue, but detection of ACE2 in the human brain, where levels are at least 20 times lower (results not

shown), was challenging. In human hippocampal sections, ACE2 was detected in NeuN-positive neurons, particularly in large ones staining weakly for DAPI and in small ones with a strong DAPI signal (Figure 5A, B). In sections of human parietal cortex, ACE2 detection was also more prominent in neuron-like cells (Figure 5C, D, E). On the other hand, in mouse sections, ACE2 staining was more intense in the cerebrovasculature and colocalized neatly with PDGFRß, indicating an expression in mouse pericytes (Figure 5F-H). These results are consistent with Western blot data, showing that ACE2 can be detected in neuron-like cells in the human brain, whereas it is concentrated in cerebrovascular cells in the mouse.

Microvascular and whole-brain ACE2 protein levels are not altered in a mouse model of AD

To probe whether changes in ACE2 could be a consequence of classical tau and Aβ neuropathology, we used the triple transgenic mouse model of AD (3xTg-AD) [59], which develops Aβ plaques and neurofibrillary tangles by 12 months of age. We quantified ACE2 protein levels in both 3xTg-AD and non-transgenic mice from two different cohorts: (i) mice of 4 or 6, 12, and 18 months of age, (ii) and 18-month-old mice fed either a control or a HFD that exacerbates neuropathology [76] (Figure 6). No significant change was observed in protein levels of ACE2 in TBS-soluble or detergent-soluble fractions according to genotype and age (Figure 6A). Similarly, ACE2 in cerebrovascular fractions did not vary according to genotype, age, and diet (Figure 6B). These results suggest that the development of human tau and Aβ neuropathology in mice is insufficient to increase murine ACE2 levels, even when combined with aging and HFD, two risk factors for AD and COVID-19 infection.

Discussion

This present *postmortem* study investigated ACE2 concentrations in the brain of individuals with AD from two different cohorts. We assessed ACE2 protein levels in all subjects and mRNA expression in a subset. We observed a significant relationship between ACE2 levels, the neuropathological diagnosis of AD, and *antemortem* cognitive evaluation. Overall, our data indicate that (1) levels of TBS-soluble ACE2 in the parietal cortex were higher in persons with AD when compared to control subjects, accompanied by an elevation in ACE2 mRNA transcripts; (2) lower cognitive scores were associated with higher levels of ACE2 in TBS-soluble and cerebrovascular fractions; (3) an apparent transfer of ACE2 from membranes to soluble compartment was associated with pericyte loss and other markers of AD progression; (4) ACE2 levels remained unchanged in an animal model of AD-like neuropathology; (5) whereas ACE2 was concentrated in microvessels in the mouse brain, it was predominantly located in neurons in the human brain. Such a series of observations highlight that an AD diagnosis is associated with higher levels of specific forms of ACE2 in the brain, which might contribute to the higher risk of SARS-CoV-2 CNS infection in cognitively impaired individuals.

Higher levels of soluble ACE2 are associated with AD and cognitive decline.

The present observation of higher levels of soluble ACE2 in AD is in agreement with a previous report using a limited number of hippocampal samples of AD subjects (n = 13) compared to Controls (n = 5) [17]. Furthermore, preliminary human brain microarray data mentioned in a letter to the Editor also cite higher ACE2 expression levels in AD patient [47]. Although an association between SARS-CoV-2 infection and cognitive impairment has been previously evidenced at the population level [79] and hinted by genetic studies [25, 42], a significant correlation between ACE2 in the brain and cognitive scores has not been reported previously.

Several mechanisms could explain the higher levels of ACE2 in AD. Since old age increases the risk of infection with SARS-CoV-2 and developing cognitive decline and AD, we could have expected an association between cerebral ACE2 levels and advanced age. However, no correlation between age and ACE2 could be evidenced here in both human and mouse samples, suggesting that changes in TBS-soluble ACE2 are not directly related to age but rather to AD pathology and cognitive decline. This is consistent with health records data showing that dementia is associated with a higher risk for COVID-19, independently of age [79]. Indeed, a recent network analysis suggest that AD and COVID-19 share defects in neuroinflammation and microvascular injury pathways [90]. Second, the increase in ACE2 could be a consequence of the AD neurodegenerative process and/or of potential compensatory mechanisms in response to AD neuropathology, which could include an increase in gene transcription, which is consistent with the higher mRNA expression measured in AD samples. However, data gathered in 3xTg-AD mice do not fully support that hypothesis. Indeed, the accumulation of human Aβ peptides and hyperphosphorylated tau in this mouse model did not lead to changes in murine ACE2 protein levels, suggesting that an ACE2 increase is not a consequence of classical AD neuropathology. Nevertheless, it should be reminded that such a mouse model displays an amount of Aβ and tau 1 to 3 logs lower than what is typically found in an AD brain. Moreover, ACE2 pathways may simply be regulated differently in the mouse, as suggested by the different localization of the protein in the murine brain.

ACE2 is part of the renin angiotensin system (RAS), which regulates the vascular system. An increase of cerebral ACE2 may impact the brain RAS, thereby affecting blood flow, arterial pressure, neuroinflammation and, consequently, brain function. Such a dysregulation of the RAS-equilibrium in the brain could contribute to the aetiology of several neurodegenerative diseases, including AD [2, 80, 81]. For example, in a cohort study including community-dwelling older

adults with mild to moderate AD, the use of ACE inhibitors (ACEi) was associated with a slower cognitive decline, independent from their antihypertensive effects [69]. ACEi and angiotensin II receptor blockers (ARBs) are also under investigation to improve cognitive impairment associated with AD [24, 27, 37, 65]. Moreover, twice higher soluble ACE2 has been reported in the cerebrospinal fluid of hypertensive patients [83]. In our study, we did not detect any association with the use of drugs acting on ACE, such as ARBS or ACEi, and brain levels of ACE2, but the study was not designed for that purpose. However, it is important to note that the levels of ACE2 detected by immunoblotting may not directly inform on ACE2 activity. Indeed, a *postmortem* assessment of ACE2 enzymatic activity with a fluorogenic assay instead showed a reduction in AD [43]. Studies in animals indicate that pharmacological activation of ACE2 rather reduces hippocampal soluble Aβ and reverses cognitive impairment in the Tg2576 model of Aβ neuropathology [22].

Another peculiar observation is the difference between ACE2 found in soluble fractions containing cytoplasmic/extracellular proteins *versus* ACE2 retrieved in detergent-soluble fractions containing membrane-bound proteins. Overall, ACE2 in TBS-soluble fractions was higher in subjects with AD, while no such trend was observed with ACE2 located in membranes. Moreover, the correlation between ACE2 and AD-relevant markers, most notably the pericyte markers PDGFRβ and others like ANPEP, differed significantly between the two fractions. The strong inverse association with TDP-43 pathology was also limited to detergent-soluble ACE2. Previous studies did not distinguish TBS-soluble *versus* detergent-soluble ACE2 [17, 47]. Although ACE2 is generally considered a membrane protein, its actual attachment to the cytoplasm membrane is relatively weak. For example, the ACE2 ectodomain can be cleaved by ADAM17 or TMPRSS2 and released in the cytoplasm [35, 91]. Recent studies report that a decrease in active membrane-bound ACE2 due to

ADAM17 and TMPRSS2 overactivation could be deleterious for SARS-CoV-2-infected patients [35, 60, 82]. However, we did not observe differences in mRNA and protein levels of TMPRSS2. Vascular ACE2 was also specifically measured in this study. Despite associations with cognitive scores and PDGFRβ levels, no significant difference was detected between groups, possibly due to the interindividual variability induced by the separation process. An intriguing possibility explaining the higher content in ACE2 specific in the TBS fraction, as detected with an antibody targeting the N-terminal extracellular domain, could be an enhanced release of ACE2 from the membrane to the cytosol or the extracellular parenchyma in AD, also termed ACE2 shedding [35, 78]. Such a detachment of ACE2 from cell membranes may be a pathological phenomenon associated with AD, warranting further study.

The present work also unveils additional information on the cellular localization of ACE2 in the human brain. While we observed an enrichment of ACE2 in mouse microvessels, such was not the case in human samples. ACE2 was detected in human samples using Western blot and RT-qPCR, but a clear immunofluorescence signal was more challenging to achieve. Unlike in the mouse, where the enrichment in microvessels was evident, the detection of ACE2 in human brain capillaries became apparent only after microvascular fractionation. However, ACE2 was clearly present in neurons in human brain sections, corroborating Western blot results. Nonetheless, it should be noted that brains from mice were harvested quickly after transcardial perfusion. On the other hand, human brain tissue underwent *premortem* and *postmortem* events, which may have affected ACE2 distribution and detection. In sum, the present data obtained using several different antibodies indicate that the cerebral distribution of ACE2 is less strictly vascular, more neuronal in humans compared to the mouse. At the very least, work related to human ACE2 but performed in

mouse models should be interpreted with caution regarding their possible application to the brain RAS, AD and other neuropathologies, as well as central SARS-CoV-2 infection in humans.

Conclusions

In summary, the present data show an accumulation of the soluble form of ACE2 associated with cognitive decline in individuals with a neuropathological diagnosis of AD. ACE2 levels were not influenced by age or biological sex. We also observed a strong association between soluble ACE2 levels and AD neuropathology, as well as pericyte loss. The search for molecular cues that cause a rise of TBS-soluble ACE2 and regulate the brain RAS in AD subjects may ultimately lead to the discovery of new therapeutics to prevent cognitive decline and AD.

List of Abbreviations

ACEi = Angiotension I Converting Enzyme Inhibitors; ACE2 = Angiotensin I Converting Enzyme 2; AD = Alzheimer's disease; ARBs = Angiotensin II receptors blockers; BA = Brodmann area; BBB = Blood brain barrier; CD = control diet; CNS = Central Nervous System; COVID-19 =Coronavirus disease 2019; DAPI = 4′,6-diamidino-2-phenylindole; EHR = electronic health records; FFPE = formalin-fixed, paraffin-embedded; GWAS = genome wide associations study; HRP = horseradish peroxidase; HFD = High fat diet; MCI = Mild-cognitive impairment; NIA-AA = National Institute of Aging – Alzheimer's Association NCI = No cognitive impairment; O.D. = Optical density; RBD = Receptor Binding Domain; NHS = Normal Horse Serum; PBS = phosphate-buffered saline; pCAA = parenchymal cerebral angiopathy amyloid; PDGFRβ = Platelet-derived growth factor receptor β; ROS = Religious Order Study; SARS-CoV-2 =Severe Acute Respiratory Syndrome CoronaVirus 2; SDS-PAGE = sodium dodecyl sulphate-

polyacrylamide gel electrophoresis; TBS = Tris-Buffered Saline; TMPRSS2 = Transmembrane protease serine 2.

Declarations

Ethics approval and consent to participate

All procedures performed with volunteers included in this study were in accordance with the ethical standards of the institutional ethics committees and with the 1964 Helsinki Declaration. Written informed consent was obtained from all individual participants included in this study. All procedures relating to mouse care and experimental treatments were approved by the Laval University animal research committee (CPAUL) in accordance with the standards of the Canadian Council on Animal Care.

Consent for publication

Not applicable.

Availability of data and material

The datasets analysed during the current study available from the corresponding author on reasonable request. Data from the ROS can be requested at https://www.radc.rush.edu.

Competing interests

The authors report no competing interests.

Funding

Funding was provided by the Canadian Institutes of Health Research (CIHR) (MOP 125930) and by The Canadian Consortium on Neurodegeneration in Aging (CCNA) to F.C. The study was

supported in part by P30AG10161, P30AG72975, R01AG15819, and R01AG58639 (D.A.B). F.C is a Fonds de recherche du Quebec - Sante (FRQ-S) senior research scholar.

Authors' contributions

LR, VE, SH, and FC designed the study. LR, ML, VE, AL, PB, and CT performed experiments. DAB provided ROS samples. LR and FC analyzed data. LR, VE and FC wrote the first drafts of the paper.

Acknowledgements

We thank Dr Pierre Leclerc from CRCHU de Québec – Université Laval for providing human FFPE testis samples. The authors are indebted to the nuns, priests and brothers from the Catholic clergy participating in the Religious Orders Study.

Supplementary material

Supplementary material is available online.

References

1 Abdi A, Jalilian M, Sarbarzeh PA, Vlaisavljevic Z (2020) Diabetes and COVID-19: A systematic review on the current evidences. Diabetes Research and Clinical Practice. Elsevier Ireland Ltd, City

2 Abiodun OA, Ola MS (2020) Role of brain renin angiotensin system in neurodegeneration: An update. Saudi Journal of Biological Sciences. Elsevier B.V., City, pp 905-912

3 Alnefeesi Y, Siegel A, Lui LMW, Teopiz KM, Ho RCM, Lee Y, Nasri F, Gill H, Lin K, Cao Bet al (2020) Impact of SARS-CoV-2 Infection on Cognitive Function: A Systematic Review. Front Psychiatry 11: 621773 Doi 10.3389/fpsyt.2020.621773

4 Barron AM, Rosario ER, Elteriefi R, Pike CJ (2013) Sex-Specific Effects of High Fat Diet on Indices of Metabolic Syndrome in 3xTg-AD Mice: Implications for Alzheimer's Disease. PLoS ONE. PLoS One, City

5 Bennett DA, A. Schneider J, Arvanitakis Z, S. Wilson R (2012) Overview and Findings from the Religious Orders Study. Current Alzheimer Research. Bentham Science Publishers Ltd., City, pp 628-645

6 Bennett DA, Buchman AS, Boyle PA, Barnes LL, Wilson RS, Schneider JA (2018) Religious Orders Study and Rush Memory and Aging Project. Journal of Alzheimer's Disease. IOS Press, City, pp S161-S189

7 Bennett DA, Wilson RS, Schneider JA, Evans DA, Beckett LA, Aggarwal NT, Barnes LL, Fox JH, Bach J (2002) Natural history of mild cognitive impairment in older persons. Neurology. Lippincott Williams and Wilkins, City, pp 198-205

8 Beyrouti R, Adams ME, Benjamin L, Cohen H, Farmer SF, Goh YY, Humphries F, Jäger HR, Losseff NA, Perry RJet al (2020) Characteristics of ischaemic stroke associated with COVID-19. Journal of Neurology, Neurosurgery and Psychiatry. BMJ Publishing Group, City

9 Bories C, Guitton MJ, Julien C, Tremblay C, Vandal M, Msaid M, de Koninck Y, Calon F (2012) Sex-Dependent Alterations in Social Behaviour and Cortical Synaptic Activity Coincide at Different Ages in a Model of Alzheimer's Disease. PLoS ONE. PLoS One, City

10 Bourassa P, Alata W, Tremblay C, Paris-Robidas S, Calon F (2019) Transferrin Receptor-Mediated Uptake at the Blood-Brain Barrier Is Not Impaired by Alzheimer's Disease Neuropathology. Molecular pharmaceutics, City, pp 583-594

11 Bourassa P, Tremblay C, Schneider JA, Bennett DA, Calon F (2019) Beta-amyloid pathology in human brain microvessel extracts from the parietal cortex: relation with cerebral amyloid angiopathy and Alzheimer’s disease. Acta Neuropathologica. Springer Berlin Heidelberg, City, pp 801-823

12 Bourassa P, Tremblay C, Schneider JA, Bennett DA, Calon F (2020) Brain mural cell loss in the parietal cortex in Alzheimer’s disease correlates with cognitive decline and TDP-43 pathology. Neuropathology and Applied Neurobiology. Blackwell Publishing Ltd, City, pp 458-477

13 Braak H, Braak E (1991) Neuropathological stageing of Alzheimer-related changes. Acta Neuropathologica. Springer-Verlag, City, pp 239-259

14 Carrillo-Larco RM, Altez-Fernandez C (2020) Anosmia and dysgeusia in COVID-19: A systematic review. Wellcome Open Research. F1000 Research Ltd, City

15 Chen R, Wang K, Yu J, Howard D, French L, Chen Z, Wen C, Xu Z (2021) The Spatial and Cell-Type Distribution of SARS-CoV-2 Receptor ACE2 in the Human and Mouse Brains. Front Neurol 11: 573095 Doi 10.3389/fneur.2020.573095

16 Dal-Pan A, Dudonné S, Bourassa P, Bourdoulous M, Tremblay C, Desjardins Y, Calon F (2016) Cognitive-enhancing effects of a polyphenols-rich extract from fruits without changes in neuropathology in an animal model of Alzheimer's disease. Journal of Alzheimer's Disease. IOS Press, City, pp 115-135

17 Ding Q, Shults NV, Gychka SG, Harris BT, Suzuki YJ (2021) Protein Expression of Angiotensin-Converting Enzyme 2 (ACE2) is Upregulated in Brains with Alzheimer's Disease. Int J Mol Sci 22: Doi 10.3390/ijms22041687

18 Ding Y, He L, Zhang Q, Huang Z, Che X, Hou J, Wang H, Shen H, Qiu L, Li Zet al (2004) Organ distribution of severe acute respiratory syndrome (SARS) associated coronavirus (SARS-CoV) in SARS patients: Implications for pathogenesis virus transmission pathways. Journal of Pathology. J Pathol, City, pp 622-630

19 Donoghue M, Hsieh F, Baronas E, Godbout K, Gosselin M, Stagliano N, Donovan M, Woolf B, Robison K, Jeyaseelan Ret al (2000) A novel angiotensin-converting enzyme-related carboxypeptidase (ACE2) converts angiotensin I to angiotensin 1-9. Circulation research. Circ Res, City

20 Doobay MF, Talman LS, Obr TD, Tian X, Davisson RL, Lazartigues E (2007) Differential expression of neuronal ACE2 in transgenic mice with overexpression of the brain renin-angiotensin system. American Journal of Physiology - Regulatory Integrative and Comparative Physiology. Am J Physiol Regul Integr Comp Physiol, City

21 Douaud G, Lee S, Alfaro-Almagro F, Arthofer C, Wang C, McCarthy P, Lange F, Andersson JLR, Griffanti L, Duff Eet al (2022) SARS-CoV-2 is associated with changes in brain structure in UK Biobank. Nature 604: 697-707 Doi 10.1038/s41586-022-04569-5

22 Evans CE, Miners JS, Piva G, Willis CL, Heard DM, Kidd EJ, Good MA, Kehoe PG (2020) ACE2 activation protects against cognitive decline and reduces amyloid pathology in the Tg2576 mouse model of Alzheimer's disease. Acta Neuropathologica. Springer Berlin Heidelberg, City, pp 485-502

23 Eysert F, Coulon A, Boscher E, Vreulx A-C, Flaig A, Mendes T, Hughes S, Grenier-Boley B, Hanoulle X, Demiautte Fet al (2020) Alzheimer's genetic risk factor FERMT2 (Kindlin-2) controls axonal growth and synaptic plasticity in an APP-dependent manner. Molecular Psychiatry: Doi 10.1038/s41380-020-00926-w

24 Fazal K, Perera G, Khondoker M, Howard R, Stewart R (2017) Associations of centrally acting ACE inhibitors with cognitive decline and survival in Alzheimer's disease. BJPsych Open 3: 158-164 Doi 10.1192/bjpo.bp.116.004184

25 Fekih-Mrissa N, Bedoui I, Sayeh A, Derbali H, Mrad M, Mrissa R, Nsiri B (2017) Association between an angiotensin-converting enzyme gene polymorphism and Alzheimer's disease in a Tunisian population. Annals of General Psychiatry. BioMed Central Ltd., City

26 Franceschi AM, Ahmed O, Giliberto L, Castillo M (2020) Hemorrhagic Posterior Reversible Encephalopathy Syndrome as a Manifestation of COVID-19 Infection. AJNR American journal of neuroradiology. NLM (Medline), City, pp 1173-1176

27 Gebre AK, Altaye BM, Atey TM, Tuem KB, Berhe DF (2018) Targeting Renin-Angiotensin System Against Alzheimer's disease. Frontiers in Pharmacology. Frontiers Media S.A., City

28 Gu J, Gong E, Zhang B, Zheng J, Gao Z, Zhong Y, Zou W, Zhan J, Wang S, Xie Zet al (2005) Multiple organ infection and the pathogenesis of SARS. Journal of Experimental Medicine. J Exp Med, City, pp 415-424

29 Hamming I, Timens W, Bulthuis MLC, Lely AT, Navis GJ, van Goor H (2004) Tissue distribution of ACE2 protein, the functional receptor for SARS coronavirus. A first step in understanding SARS pathogenesis. Journal of Pathology. Wiley-Blackwell, City, pp 631-637

30 Harmer D, Gilbert M, Borman R, Clark KL (2002) Quantitative mRNA expression profiling of ACE 2, a novel homologue of angiotensin converting enzyme. FEBS Letters. FEBS Lett, City, pp 107-110

31 He L, Mäe MA, Muhl L, Sun Y, Pietilä R, Nahar K, Liébanas EV, Fagerlund MJ, Oldner A, Liu Jet al (2020) Pericyte-specific vascular expression of SARS-CoV-2 receptor ACE2 – implications for microvascular inflammation and hypercoagulopathy in COVID-19. bioRxiv, City, pp 2020.2005.2011.088500

32 He L, Vanlandewijck M, Mäe MA, Andrae J, Ando K, Del Gaudio F, Nahar K, Lebouvier T, Laviña B, Gouveia Let al (2018) Single-cell RNA sequencing of mouse brain and lung vascular and vessel-associated cell types. Sci Data 5: 180160 Doi 10.1038/sdata.2018.160

33 Helms J, Kremer S, Merdji H, Clere-Jehl R, Schenck M, Kummerlen C, Collange O, Boulay C, Fafi-Kremer S, Ohana Met al (2020) Neurologic features in severe SARS-COV-2 infection. New England Journal of Medicine. Massachussetts Medical Society, City, pp 2268-2270

34 Helms J, Kremer S, Merdji H, Schenck M, Severac F, Clere-Jehl R, Studer A, Radosavljevic M, Kummerlen C, Monnier Aet al (2020) Delirium and encephalopathy in severe COVID-19: a cohort analysis of ICU patients. Critical care (London, England). Crit Care, City, pp 491

35 Heurich A, Hofmann-Winkler H, Gierer S, Liepold T, Jahn O, Pohlmann S (2014) TMPRSS2 and ADAM17 Cleave ACE2 Differentially and Only Proteolysis by TMPRSS2 Augments Entry Driven by the Severe Acute Respiratory Syndrome Coronavirus Spike Protein. Journal of Virology. American Society for Microbiology, City, pp 1293-1307

36 Hikmet F, Méar L, Edvinsson Å, Micke P, Uhlén M, Lindskog C (2020) The protein expression profile of ACE2 in human tissues. Mol Syst Biol 16: e9610 Doi 10.15252/msb.20209610

37 Ho JK, Nation DA (2017) Memory is preserved in older adults taking AT1 receptor blockers. Alzheimer's Research and Therapy. BioMed Central Ltd., City

38 Hoffmann M, Kleine-Weber H, Schroeder S, Krüger N, Herrler T, Erichsen S, Schiergens TS, Herrler G, Wu NH, Nitsche Aet al (2020) SARS-CoV-2 Cell Entry Depends on ACE2 and TMPRSS2 and Is Blocked by a Clinically Proven Protease Inhibitor. Cell. Cell Press, City, pp 271-280.e278

39 Hosp JA, Dressing A, Blazhenets G, Bormann T, Rau A, Schwabenland M, Thurow J, Wagner D, Waller C, Niesen WDet al (2021) Cognitive impairment and altered cerebral glucose metabolism in the subacute stage of COVID-19. Brain 144: 1263-1276 Doi 10.1093/brain/awab009

40 Jordan RE, Adab P, Cheng KK (2020) Covid-19: Risk factors for severe disease and death. The BMJ. BMJ Publishing Group, City

41 Julien C, Tremblay C, Phivilay A, Berthiaume L, Émond V, Julien P, Calon F (2010) High-fat diet aggravates amyloid-beta and tau pathologies in the 3xTg-AD mouse model. Neurobiology of Aging. Neurobiol Aging, City, pp 1516-1531

42 Kauwe JSK, Bailey MH, Ridge PG, Perry R, Wadsworth ME, Hoyt KL, Staley LA, Karch CM, Harari O, Cruchaga Cet al (2014) Genome-Wide Association Study of CSF Levels of 59 Alzheimer's Disease Candidate Proteins: Significant Associations with Proteins Involved in Amyloid Processing and Inflammation. PLoS Genetics. Public Library of Science, City

43 Kehoe PG, Wong S, Al Mulhim N, Palmer LE, Miners JS (2016) Angiotensin-converting enzyme 2 is reduced in Alzheimer's disease in association with increasing amyloid-β and tau pathology. Alzheimer's Research and Therapy. BioMed Central Ltd., City

44 Korczyn AD (2020) Dementia in the COVID-19 Period. Journal of Alzheimer's Disease. IOS Press BV, City, pp 1253-1261

45 Lan J, Ge J, Yu J, Shan S, Zhou H, Fan S, Zhang Q, Shi X, Wang Q, Zhang Let al (2020) Structure of the SARS-CoV-2 spike receptor-binding domain bound to the ACE2 receptor. Nature. Nature Research, City, pp 215-220

46 Lee DJ, Lockwood J, Das P, Wang R, Grinspun E, Lee JM (2020) Self-reported anosmia and dysgeusia as key symptoms of coronavirus disease 2019. CJEM. Cambridge University Press (CUP), City, pp 1-8

47 Lim KH, Yang S, Kim SH, Joo JY (2020) Elevation of ACE2 as a SARS-CoV-2 entry receptor gene expression in Alzheimer's disease. Journal of Infection, City, pp e33-e34

48 Mahammedi A, Saba L, Vagal A, Leali M, Rossi A, Gaskill M, Sengupta S, Zhang B, Carriero A, Bachir Set al (2020) Imaging in Neurological Disease of Hospitalized COVID-19 Patients: An Italian Multicenter Retrospective Observational Study. Radiology. Radiological Society of North America (RSNA), City, pp 201933

49 Mao L, Jin H, Wang M, Hu Y, Chen S, He Q, Chang J, Hong C, Zhou Y, Wang Det al (2020) Neurologic Manifestations of Hospitalized Patients with Coronavirus Disease 2019 in Wuhan, China. JAMA Neurology. American Medical Association, City

50 Martín-Jiménez P, Muñoz-García MI, Seoane D, Roca-Rodríguez L, García-Reyne A, Lalueza A, Maestro G, Folgueira D, Blanco-Palmero VA, Herrero-San Martín Aet al (2020) Cognitive Impairment Is a Common Comorbidity in Deceased COVID-19 Patients: A Hospital-Based Retrospective Cohort Study. J Alzheimers Dis 78: 1367-1372 Doi 10.3233/jad-200937

51 McCracken IR, Saginc G, He L, Huseynov A, Daniels A, Fletcher S, Peghaire C, Kalna V, Andaloussi-Mäe M, Muhl Let al (2021) Lack of Evidence of Angiotensin-Converting Enzyme 2 Expression and Replicative Infection by SARS-CoV-2 in Human Endothelial Cells. Circulation 143: 865-868 Doi 10.1161/circulationaha.120.052824

52 Meng X, Deng Y, Dai Z, Meng Z (2020) COVID-19 and anosmia: A review based on up-to-date knowledge. American Journal of Otolaryngology - Head and Neck Medicine and Surgery. W.B. Saunders, City, pp 102581

53 Miners JS, Schulz I, Love S (2018) Differing associations between Aβ accumulation, hypoperfusion, blood–brain barrier dysfunction and loss of PDGFRB pericyte marker in the precuneus and parietal white matter in Alzheimer's disease. Journal of Cerebral Blood Flow and Metabolism. SAGE Publications Ltd, City, pp 103-115

54 Miners S, Kehoe PG, Love S (2020) Cognitive impact of COVID-19: looking beyond the short term. Alzheimer's Research and Therapy. BioMed Central Ltd, City

55 Mirra SS, Heyman A, McKeel D, Sumi SM, Crain BJ, Brownlee LM, Vogel FS, Hughes JP, van Belle G, Berg Let al (1991) The consortium to establish a registry for Alzheimer’s disease (CERAD). Part II. Standardization of the neuropathologic assessment of Alzheimer’s disease. Neurology. Neurology, City, pp 479-486

56 Montine TJ, Phelps CH, Beach TG, Bigio EH, Cairns NJ, Dickson DW, Duyckaerts C, Frosch MP, Masliah E, Mirra SSet al (2012) National institute on aging-Alzheimer's association guidelines for the neuropathologic assessment of Alzheimer's disease: A practical approach. Acta Neuropathologica. Acta Neuropathol, City, pp 1-11

57 Muhl L, He L, Sun Y, Andaloussi Mäe M, Pietilä R, Liu J, Genové G, Zhang L, Xie Y, Leptidis Set al (2022) The SARS-CoV-2 receptor ACE2 is expressed in mouse pericytes but not endothelial cells: Implications for COVID-19 vascular research. Stem Cell Reports 17: 1089-1104 Doi 10.1016/j.stemcr.2022.03.016

58 Mukerji SS, Solomon IH (2021) What can we learn from brain autopsies in COVID-19? Neurosci Lett 742: 135528 Doi 10.1016/j.neulet.2020.135528

59 Oddo S, Caccamo A, Shepherd JD, Murphy MP, Golde TE, Kayed R, Metherate R, Mattson MP, Akbari Y, LaFerla FM (2003) Triple-transgenic model of Alzheimer's Disease with plaques and tangles: Intracellular Aβ and synaptic dysfunction. Neuron. Cell Press, City, pp 409-421

60 Palau V, Riera M, Soler MJ (2020) ADAM17 inhibition may exert a protective effect on COVID-19. Nephrology Dialysis Transplantation. Oxford University Press, City, pp 1071-1072

61 Paterson RW, Brown RL, Benjamin L, Nortley R, Wiethoff S, Bharucha T, Jayaseelan DL, Kumar G, Raftopoulos RE, Zambreanu Let al (2020) The emerging spectrum of COVID-19 neurology: clinical, radiological and laboratory findings. Brain : a journal of neurology, City

62 Perrotta F, Corbi G, Mazzeo G, Boccia M, Aronne L, D’Agnano V, Komici K, Mazzarella G, Parrella R, Bianco A (2020) COVID-19 and the elderly: insights into pathogenesis and clinical decision-making. Aging Clinical and Experimental Research. Springer, City, pp 1599-1608

63 Pugazhenthi S, Qin L, Reddy PH (2017) Common neurodegenerative pathways in obesity, diabetes, and Alzheimer's disease. Biochimica et Biophysica Acta (BBA) - Molecular Basis of Disease, City, pp 1037-1045

64 Rhea EM, Logsdon AF, Hansen KM, Williams LM, Reed MJ, Baumann KK, Holden SJ, Raber J, Banks WA, Erickson MA (2020) The S1 protein of SARS-CoV-2 crosses the blood–brain barrier in mice. Nature Neuroscience. Nature Research, City

65 Ribeiro VT, de Souza LC, Simões e Silva AC (2019) Renin-Angiotensin System and Alzheimer's Disease Pathophysiology: From the Potential Interactions to Therapeutic Perspectives. Protein & Peptide Letters. Bentham Science Publishers Ltd., City, pp 484-511

66 Rizzo MR, Paolisso G (2021) SARS-CoV-2 Emergency and Long-Term Cognitive Impairment in Older People. Aging Dis 12: 345-352 Doi 10.14336/ad.2021.0109

67 Roca-Ho H, Riera M, Palau V, Pascual J, Soler MJ (2017) Characterization of ACE and ACE2 expression within different organs of the NOD mouse. International Journal of Molecular Sciences. MDPI AG, City

68 Sah SK, Lee C, Jang JH, Park GH (2017) Effect of high-fat diet on cognitive impairment in triple-transgenic mice model of Alzheimer's disease. Biochemical and Biophysical Research Communications. Elsevier B.V., City, pp 731-736

69 Soto ME, Abellan Van Kan G, Nourhashemi F, Gillette-Guyonnet S, Cesari M, Cantet C, Rolland Y, Vellas B (2013) Angiotensin-converting enzyme inhibitors and alzheimer's disease progression in older adults: Results from the Réseau sur la Maladie d'Alzheimer Français cohort. Journal of the American Geriatrics Society. J Am Geriatr Soc, City, pp 1482-1488

70 St-Amour I, Paré I, Tremblay C, Coulombe K, Bazin R, Calon F (2014) IVIg protects the 3xTg-AD mouse model of Alzheimer's disease from memory deficit and A?? pathology. Journal of Neuroinflammation, City, pp 1-16

71 Stein SR, Ramelli SC, Grazioli A, Chung J-Y, Singh M, Yinda CK, Winkler CW, Sun J, Dickey JM, Ylaya Ket al (2022) SARS-CoV-2 infection and persistence in the human body and brain at autopsy. Nature: Doi 10.1038/s41586-022-05542-y

72 Thal DR, Rüb U, Orantes M, Braak H (2002) Phases of Aβ-deposition in the human brain and its relevance for the development of AD. Neurology. Lippincott Williams and Wilkins, City, pp 1791-1800

73 Tipnis SR, Hooper NM, Hyde R, Karran E, Christie G, Turner AJ (2000) A human homolog of angiotensin-converting enzyme: Cloning and functional expression as a captopril-insensitive carboxypeptidase. Journal of Biological Chemistry. J Biol Chem, City, pp 33238-33243

74 Tremblay C, François A, Delay C, Freland L, Vandal M, Bennett DA, Calon F (2017) Association of Neuropathological Markers in the Parietal Cortex With Antemortem Cognitive Function in Persons With Mild Cognitive Impairment and Alzheimer Disease. Journal of neuropathology and experimental neurology, City, pp 70-88

75 Tremblay C, St-Amour I, Schneider J, Bennett DA, Calon F (2011) Accumulation of transactive response DNA binding protein 43 in mild cognitive impairment and Alzheimer disease. Journal of Neuropathology and Experimental Neurology. J Neuropathol Exp Neurol, City, pp 788-798

76 Vandal M, White PJ, Tremblay C, St-Amour I, Chevrier G, Emond V, Lefranc¸ois D, Virgili J, Planel E, Giguere Yet al (2014) Insulin reverses the high-fat diet-induced increase in brain Aβ and improves memory in an animal model of Alzheimer disease. Diabetes, City, pp 4291-4301

77 Vanlandewijck M, He L, Mäe MA, Andrae J, Ando K, Del Gaudio F, Nahar K, Lebouvier T, Laviña B, Gouveia Let al (2018) A molecular atlas of cell types and zonation in the brain vasculature. Nature 554: 475-480 Doi 10.1038/nature25739

78 Wang J, Zhao H, An Y (2022) ACE2 Shedding and the Role in COVID-19. Frontiers in Cellular and Infection Microbiology 11: Doi 10.3389/fcimb.2021.789180

79 Wang Q, Davis PB, Gurney ME, Xu R (2021) COVID-19 and dementia: Analyses of risk, disparity, and outcomes from electronic health records in the US. Alzheimer's & Dementia. Wiley, City

80 Wright JW, Harding JW (2019) Contributions by the brain renin-angiotensin system to memory, cognition, and Alzheimer's disease. Journal of Alzheimer's Disease. IOS Press, City, pp 469-480

81 Wright JW, Kawas LH, Harding JW (2013) A Role for the Brain RAS in Alzheimer's and Parkinson's Diseases. Frontiers in Endocrinology. Frontiers Media SA, City

82 Xiao L, Sakagami H, Miwa N (2020) ACE2: The key molecule for understanding the pathophysiology of severe and critical conditions of COVID-19: Demon or angel? Viruses. MDPI AG, City

83 Xu J, Sriramula S, Xia H, Moreno-Walton L, Culicchia F, Domenig O, Poglitsch M, Lazartigues E (2017) Clinical Relevance and Role of Neuronal AT1 Receptors in ADAM17-Mediated ACE2 Shedding in Neurogenic Hypertension. Circulation Research. Lippincott Williams and Wilkins, City, pp 43-55

84 Yang AC, Vest RT, Kern F, Lee DP, Agam M, Maat CA, Losada PM, Chen MB, Schaum N, Khoury Net al (2022) A human brain vascular atlas reveals diverse mediators of Alzheimer's risk. Nature 603: 885-892 Doi 10.1038/s41586-021-04369-3

85 Yang F, Zhao H, Liu H, Wu X, Li Y (2021) Manifestations and mechanisms of central nervous system damage caused by SARS-CoV-2. Brain Res Bull 177: 155-163 Doi 10.1016/j.brainresbull.2021.09.015

86 Yuki K, Fujiogi M, Koutsogiannaki S (2020) COVID-19 pathophysiology: A review. Clinical Immunology. Academic Press Inc., City, pp 108427

87 Zanin L, Saraceno G, Panciani PP, Renisi G, Signorini L, Migliorati K, Fontanella MM (2020) SARS-CoV-2 can induce brain and spine demyelinating lesions. Acta Neurochirurgica. Springer, City, pp 1491-1494

88 Zhang L, Zhou L, Bao L, Liu J, Zhu H, Lv Q, Liu R, Chen W, Tong W, Wei Qet al (2021) SARS-CoV-2 crosses the blood–brain barrier accompanied with basement membrane disruption without tight junctions alteration. Signal Transduction and Targeted Therapy 6: 337 Doi 10.1038/s41392-021-00719-9

89 Zhang Y, Chen K, Sloan SA, Bennett ML, Scholze AR, Keeffe S, Phatnani HP, Guarnieri P, Caneda C, Ruderisch Net al (2014) An RNA-Sequencing Transcriptome and Splicing Database of Glia, Neurons, and Vascular Cells of the Cerebral Cortex. The Journal of Neuroscience 34: 11929 Doi 10.1523/JNEUROSCI.1860-14.2014

90 Zhou Y, Xu J, Hou Y, Leverenz JB, Kallianpur A, Mehra R, Liu Y, Yu H, Pieper AA, Jehi Let al (2021) Network medicine links SARS-CoV-2/COVID-19 infection to brain microvascular injury and neuroinflammation in dementia-like cognitive impairment. Alzheimer's Research & Therapy 13: 110 Doi 10.1186/s13195-021-00850-3

91 Zipeto D, Palmeira JdF, Argañaraz GA, Argañaraz ER (2020) ACE2/ADAM17/TMPRSS2 Interplay May Be the Main Risk Factor for COVID-19. Frontiers in Immunology 11: Doi 10.3389/fimmu.2020.576745

Legends

Figure 1: Levels of TBS-Soluble ACE2 protein are higher in AD individuals and are negatively correlated with global cognitive score. Parietal cortex levels of ACE2 protein from Cohort #1 were determined by Western Blot in three fractions: a TBS-soluble fraction (A-D), a detergent-soluble fraction (E-H) and a microvessel-enriched fraction (I-L). No statistical difference was detected for ACE2 in the three fractions when subjects were classified according to *antemortem* clinical diagnosis (B, F, J). Levels of the ACE2 protein were higher in the TBS-soluble fraction in individuals with a neuropathological diagnosis of AD based on ABC scoring (C, G, K). TBS-soluble ACE2 and microvascular ACE2 levels were negatively correlated with the global cognitive score (D, L). An equal amount (12 µg) of proteins per sample for both TBS-soluble and detergent soluble fractions was loaded and 8 µg of proteins per sample was loaded for microvessel-enriched fractions. All samples, loaded in a random order, were run on the same gel and transferred on the same membrane before immunoblotting for quantification. Examples were taken from the same experiment, and consecutive bands loaded in random order are shown. Actin and cyclophilin B are shown as loading controls. Data are represented as a scatterplot. Horizontal lines indicate mean ± SEM. Statistical analysis: Mann-Whitney test **$p < 0.01$, Coefficient of determination &$p < 0.05$. *Abbreviations: ACE2, Angiotensin-Converting Enzyme 2; A/AD, Alzheimer's disease; C, control; Clin Dx, clinical diagnosis; ABC Dx, ABC neuropathological diagnosis; CyB, cyclophilin B; M/MCI, mild cognitive impairment; N/NCI, healthy controls with no cognitive impairment; O.D., optical density; TBS, Tris-Buffered Saline.*

Figure 2: Higher ACE2 protein and mRNA levels in parietal cortex of AD participants from the second cohort. AD subjects from Cohort #2 had higher levels of ACE2 protein and mRNA compared to controls. Diagnosis was determined using Braak staging. ACE2 levels were determined by Western-Blot and qPCR analysis (A, B). Statistical analysis: Mann-Whitney test *$p < 0.05$, Unpaired t-test **$p < 0.01$. All samples, loaded in a random order, were run on the same immunoblot experiment for quantification. Examples were taken from the same immunoblot experiment, and consecutive bands loaded in random order are shown. GAPDH is shown as a loading control. Data are represented as a scatterplot. Horizontal lines indicate mean ± SEM. *Abbreviations: A, Alzheimer's disease (Braak scores III-VI); ACE2, Angiotensin-Converting Enzyme 2; C, control (Braak scores I or II); Dx, diagnostic; O.D., optical density.*

Figure 3: ACE2 protein in TBS-soluble/microvascular protein fractions show opposite relationships with detergent-soluble ACE2 when correlating with AD markers. Heat-map of hierarchical clustering analysis of correlation coefficients from partial correlation analyses with *antemortem* evaluation, neuropathological markers (soluble and insoluble proteins of the parietal cortex) and BBB markers (microvascular fractions of the parietal cortex). The significance of the correlation (inverse in blue, positive in red) between two elements is entered in the associated box. Statistical analysis: Coefficient of determination *$p < 0.05$, **$p < 0.01$ and ***$p < 0.001$. All proteins presented in these heat-maps were determined by Western-blot analysis except Aβ peptides which were quantified using ELISA. Total soluble and insoluble Tau was detected using Tau (640-680) antibody. AD2 antibody recognized Tau phosphorylated at S396. Phosphorylated TDP43 antibody recognized at pSer409/410. *Abbreviations: ABCB1, ATP Binding Cassette*

Subfamily B Member 1; ACE2, Angiotensin-Converting Enzyme 2; ANPEP, Aminopeptidase N; BBB, blood-brain barrier; BACE1, Beta-Secretase 1; CD31 or PECAM1, Platelet endothelial cell adhesion molecule; LRP1, Low density lipoprotein receptor-related protein 1; NS, non significative; PDGFRß, Platelet Derived Growth Factor Receptor Beta; RAGE, Receptor for Advanced Glycation Endproducts; αSMA, alpha smooth muscle actin; TDP-43, TAR DNA binding protein 43; TBS, Tris-Buffered Saline.

Figure 4: In fractionated brain homogenates, ACE2 immunosignal is predominantly observed in neurons in human samples and in the vasculature in mice. (A, F) Immunoblotting detection of ACE2 in human (parietal cortex) (A) and mouse (whole brain)(F) vascular fractions "*Va*", compared to postvascular parenchymal samples depleted in vascular cells "*P*" and total unfractionated homogenates "*T*". For comparison purposes, synaptophysin (a synaptic/neuronal marker), Claudin5 (endothelial marker), and PDGFRß (pericyte marker), are also shown. In the mouse brain, ACE2 is highly enriched in microvessels compared to the postvascular fraction, different to what is observed in the human (A, F). (B-E, G, H) Representative immunostaining of ACE2 (green) in human (B-E) and murine cerebrovascular fractions (G, H), with collagen IV (endothelial marker) in red (B, D, G, H) or blue (C, E), as well as NeuN (neuronal marker) in red (C, E) and DAPI (nuclei) in blue (B-H). In human samples, moderate ACE2 staining is observed in neurons, whereas vascular ACE2 staining is strong in mice. Red arrows point to ACE2+/NeuN+ cells, blue arrows to ACE2+/NeuN- cells, and green arrows to erythrocytes. ACE2 antibodies: rb mAb #ab108252 (A, F), rb pAb #HPA000288 (B, D, G) and #35-1875 (C, E, H). Scale bar: 10 µm. *Abbreviations: ACE2, Angiotensin-Converting Enzyme 2; Coll IV, Collagen IV; Coloc, Colocalization; PDGFRß, Platelet Derived Growth Factor Receptor Beta. mAb, monoclonal antibody; pAb, polyclonal antibody.*

Figure 5: In tissue sections, ACE2 immunostaining is predominantly observed in neurons in the human brain and in the cerebrovasculature in mice. (A-E) Representative immunostaining of ACE2 (green or red) in fresh frozen human hippocampus (A, B), formalin-fixed paraffin-embedded parietal cortex (C-E), and in murine fresh frozen hippocampal and cerebellar sections (F-H). For immunofluorescence, NeuN (neuronal marker)(A, B), collagen IV (endothelial marker)(F, G) or PDGFRß (pericyte marker) (H) are in red, and DAPI (nuclei) is in blue (A-C, F-H). For immunohistochemistry, sections were counterstained with hematoxylin (nuclei)(D, E), and negative control is inserted in (E). In human samples, strong ACE2 staining is observed in large and small neurons, whereas in mice, neuronal signal is moderate and vascular ACE2 staining is strong and colocalizes well with PDGFRß. Red arrows point to ACE2+/NeuN+ cells and green arrows to erythrocytes; dashed white line highlights small ACE2+/NeuN+ cells that stain strongly for DAPI. ACE2 antibodies: rabbit mAb #ab108252 (C, G), rabbit pAb #HPA000288 (A, B, E, F) and #35-1875 (D) or goat pAb #AF3437. Scale bars: 200 µm (A, F, G, H), 20 µm (B, D, E) and 10 µm (C). *Abbreviations: ACE2, Angiotensin-Converting Enzyme 2; Coll IV, Collagen IV; Coloc, Colocalization; PDGFRß, Platelet Derived Growth Factor Receptor Beta; mAb, monoclonal antibody; pAb, polyclonal antibody.*

Figure 6: ACE2 levels are not altered in a model of AD, the 3xTg-AD mouse. (A) Determination of ACE2 levels by Western immunoblotting in brain homogenates from NonTg and 3xTg-AD mice aged 4, 12, and 18 months. No difference was observed in TBS-soluble and

detergent-soluble ACE2. (B) In brain microvessel-enriched fractions from NonTg and 3xTg-AD mice aged 6, 12, 18 months, and in 18-month-old animals fed either a control diet or a high fat diet, no difference was observed in microvascular ACE2 levels. ACE2 levels in the mouse brain are not influenced by age or a diet that exacerbates AD-like neuropathology. Examples were taken from the same immunoblot experiment, and consecutive bands loaded in random order are shown. Actin and cyclophilin B are shown as loading controls. Data are represented as mean ± SEM. Statistical analysis: Kruskal-Wallis, ns, non-significant. *Abbreviations: Angiotensin-Converting Enzyme 2; Non-Tg,/NT, non-transgenic mice; 3x, 3xTg-AD mice; CD/C, control diet; CyB, cyclophilin B; HFD/H, high-fat diet; O.D., optical density.*

Table 1: Characteristics of Cohort #1 (Religious Order Study) and Cohort #2 (US other sources).

Cohort #1 characteristics (Religious Order Study): Participants were assigned to the "Control" or "AD" group based on the level of AD neuropathological changes associated with their ABC scores [70]. ABC scores were converted into one of the four levels of AD neuropathological changes (not, low, intermediate, or high) using the chart described in the revised NIA-AA guidelines [70]. Intermediate or high levels of AD neuropathological changes were assigned to the "AD" group, while those with no or a low level of AD neuropathological changes were rather assigned to the "Control" group [70]. Parenchymal CAA stages in parietal cortex were determined in the angular gyrus. Brain pH was measured in cerebellum extracts. Soluble Aβ peptide concentrations were determined by ELISA in whole homogenates of inferior parietal cortex. Values are expressed as means (SD) unless specified otherwise. Statistical analysis (compared to controls): Mann Whitney test: #p < 0.01; ¶p < 0.001; &p < 0.0001; Pearson test: £p < 0.01. Claudin5 and CD31 data in microvessel extracts were normalized with cyclophilin B as a loading control. **Cohort #2 characteristics (Other US Sources)**: Brain samples of this cohort were provided by Harvard Brain Tissue Resource Center (Boston), Miller School of Medicine (Miami) and Human Brain and Spinal Fluid Resource Center (Los Angeles). Participants were assigned to the "Control" or "AD" group based on the Braak score. Values are expressed as means (SD). Statistical analysis (compared to controls): Unpaired t test, Pearson test. *Abbreviations: AD, Alzheimer's disease; C, contingency; CAA, cerebral amyloid angiopathy; CERAD, Consortium to Establish a Registry for Alzheimer's Disease; MCI, mild cognitive impairment; MMSE, Mini-Mental State Examination; NCI, healthy controls with no cognitive impairment; ROD, relative optical density.*

Figure S1: AD subjects with parenchymal CAA have higher soluble ACE2. Individuals were grouped based on their ABC neuropathological diagnosis or clinical diagnosis and subdivided based on the presence of parenchymal CAA (pCAA). *(A)* Levels of soluble ACE2 were higher in subjects with an AD neuropathological and clinical diagnosis with the presence of pCAA. *(B)* Levels of detergent-soluble ACE2 did not change depending on the presence or absence of pCAA. All samples, loaded in a random order, were run on the same immunoblot experiment for quantification. Examples were taken from the same immunoblot experiment, and consecutive bands loaded in random order are shown. Data are represented as a scatterplot. Horizontal lines indicate mean ± SEM. Statistical analysis: two groups: unpaired t-test *p <0.05 or three groups: Tukey's multiple comparisons test *p<0.05, **p<0.01. *Abbreviations: A/AD, Alzheimer's disease;;*

C, control; Clinical Dx, clinical diagnosis; M/MCI, mild cognitive impairment; N/NCI, healthy controls with no cognitive impairment; O.D., Optical density; pCAA, parenchymal cerebral amyloid angiopathy.

Figure S2: Levels of TMPRSS2 protein, which is employed by SARS-CoV-2 for Spike protein priming, are unchanged in AD individuals. *(A)* Levels of the TMPRSS2 protein were measured in Cohort #1: no difference was identified according to clinical or neuropathological (ABC) diagnosis. *(B)* In Cohort#2, TMRPSS protein and mRNA quantification did not reveal difference between control and AD. All samples, loaded in a random order, were run on the same immunoblot experiment for quantification. Examples were taken from the same immunoblot experiment, and consecutive bands loaded in random order are shown. Data are represented as a scatterplot. Horizontal lines indicate mean ± SEM. Statistical analysis: Ordinary on-way ANOVA or Mann-Whitney test, non-significant. *Abbreviations: A/AD, Alzheimer's disease; ABC Dx, ABC neuropathological diagnosis; Braak Dx, Braak staging diagnosis; C, control; Clinical Dx, clinical diagnosis; M/MCI, mild cognitive impairment; N/NCI, healthy controls with no cognitive impairment; ROD, relative optical density; TMRPSS2, Transmembrane protease serine 2.*

Figure S3: Examples of correlation plots between ACE2 in the three protein fractions and age or AD-related proteins are shown. No significant correlation was established between ACE2 in all fractions tested and the age of death. TBS-soluble ACE2 was positively correlated with soluble Aß42 peptides and phospho-tau AD2. Both TBS-soluble and microvessel ACE2 were positively associated with microvascular RAGE but negatively with microvascular PDGFRß. Significant correlations are shown with the sign & in red. All proteins presented in these correlations were determined by Western-blot analysis except Aß peptides, which were determined using ELISA. Coefficient of determination &p < 0.05, &&p < 0.01, &&&p < 0.001. *Abbreviations: ACE2, Angiotensin-Converting Enzyme 2; AD, Alzheimer's disease; MCI, mild cognitive impairment; NCI, healthy controls with no cognitive impairment; PDGFRß, Platelet Derived Growth Factor Receptor Beta; RAGE, Receptor for Advanced Glycation Endproducts; Relative OD, relative optical density.*

Figure S4: Human formalin-fixed paraffin-embedded testis sections were used as positive controls for ACE2 immunostaining, which is strong in this tissue. Antibodies used: (A) goat pAb #PA5-4788 from ThermoFisher, (B) goat pAb #AF933 from BioTechne, (C) goat pAb #AF3437 from BioTechne, (D) mouse mAb #sc-73668 from Santa Cruz, (E) rabbit pAb #35-1875 from Abeomics, (F) rb pAB #ab15348 from Abcam, (G) mouse mAb #sc-390851 from Santa Cruz, (H) rabbit mAb #ab108252 from Abcam and (I) rabbit pAb #HPA000288 from Atlas. Scale bars: 400 µm (A-H) and 200 µm (I). *Abbreviations: ACE2, Angiotensin-Converting Enzyme 2; Coll IV, Collagen IV; mAb, monoclonal antibody; pAb, polyclonal antibody.*

Figure S5: Western blots in human TBS-soluble, detergent-soluble and microvessel-enriched extracts from Cohort#1. The clinical and neuropathological diagnoses are given above each sample. *Abbreviations: A, Alzheimer's Disease; ABC Dx, ABC neuropathological diagnosis; ACE2, Angiotensin-Converting Enzyme 2; C, Control; ClinDx, Clinical diagnosis; M, mild cognitive impairment; N, healthy controls with no cognitive impairment; TMRPSS2, Transmembrane protease serine 2.*

Figure S6: Western blots in brain homogenates from Cohort#2. Diagnosis was determined using Braak staging. *Abbreviations: A, Alzheimer's Disease; ACE2, Angiotensin-Converting Enzyme 2; Braak Dx, Braak staging diagnosis; Cal, Calibrator; C, Control*; *GAPDH, Glyceraldehyde 3-phosphate dehydrogenase; TMRPSS2, Transmembrane protease serine 2.*

Supplementary method:

Isolation of murine brain microvessels

The procedure used for isolation of murine brain microvessels has been reported in our previous work (Bourassa *et al*., 2019a). Nontransgenic and 3xTg-AD mice aged 6, 12 and 18 months were sacrificed with an intracardiac perfusion of ice-cold PBS containing 0.32 M sucrose and protease (SIGMA*FAST* Protease Inhibitor tablets, Sigma-Aldrich) and phosphatase (1 mM sodium pyrophosphate and 50 mM sodium fluoride) inhibitors, under deep anesthesia with ketamine/xylazine. The brains were immediately collected, and brainstem, cerebellum and meninges were removed. Murine brain samples were then chopped and frozen in 0.5 mL of MIB containing 0.32 M sucrose and protease and phosphatase inhibitors (Bimake). For a milder freezing we used Mr. Frosty™ Freezing Container (Thermo Scientific). The microvessel enrichment procedure was then conducted as described for human samples. To validate the enrichment of mural cell markers, the microvessel-enriched and the microvessel-depleted fractions were compared to a total brain homogenate obtained from the homogenization of a whole hemisphere of a control mouse in the lysis buffer. Protein concentrations in all fractions were determined using the bicinchoninic acid assay (Thermo Fisher Scientific)

Figure 1

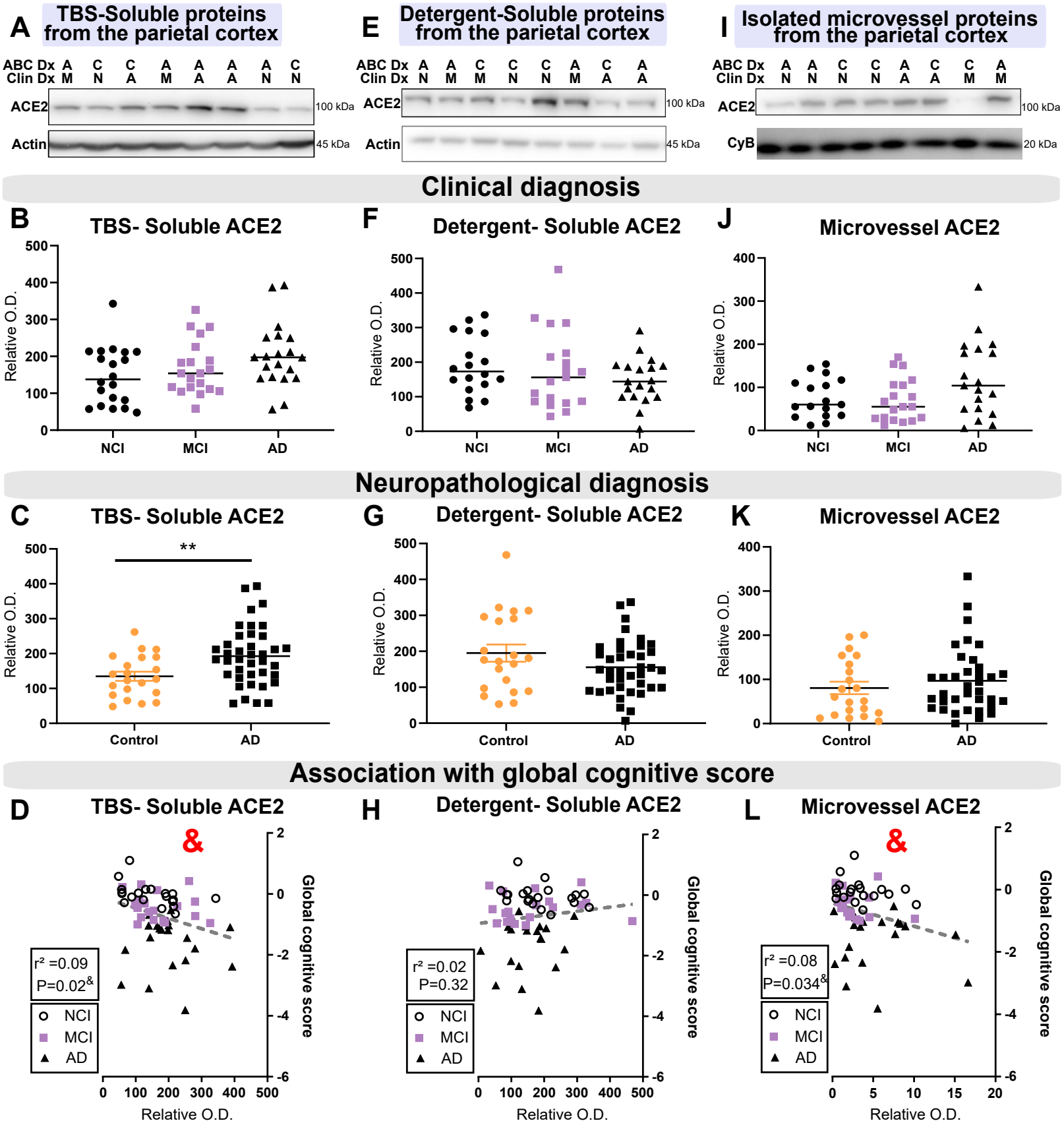
A
TBS-Soluble proteins from the parietal cortex
ABC Dx A A C C A A A A C
Clin Dx A M C N C A A M A A A N C N
ACE2
100 kDa
Actin
45 kDa
E
Detergent-Soluble proteins from the parietal cortex
ABC Dx A A A C C C A C A
Clin Dx A N A M C M C N C N A M C A A A
ACE2
100 kDa
Actin
45 kDa
I
Isolated microvessel proteins from the parietal cortex
ABC Dx A A C C A C C A
Clin Dx A N A N C N A A C A C M A M
ACE2
100 kDa
CyB
20 kDa
Clinical diagnosis
B
TBS- Soluble ACE2
Relative O.D.
NCI
MCI
AD
F
Detergent- Soluble ACE2
Relative O.D.
NCI
MCI
AD
J
Microvessel ACE2
Relative O.D.
NCI
MCI
AD
Neuropathological diagnosis
C
TBS- Soluble ACE2
**
Relative O.D.
Control
AD
G
Detergent- Soluble ACE2
Relative O.D.
Control
AD
K
Microvessel ACE2
Relative O.D.
Control
AD
Association with global cognitive score
D
TBS- Soluble ACE2
&
r² =0.09
P=0.02&
NCI
MCI
AD
Relative O.D.
Global cognitive score
H
Detergent- Soluble ACE2
r² =0.02
P=0.32
NCI
MCI
AD
Relative O.D.
Global cognitive score
L
Microvessel ACE2
&
r² =0.08
P=0.034&
NCI
MCI
AD
Relative O.D.
Global cognitive score

Figure 2

Quantification of ACE2 in the parietal cortex from Cohort #2

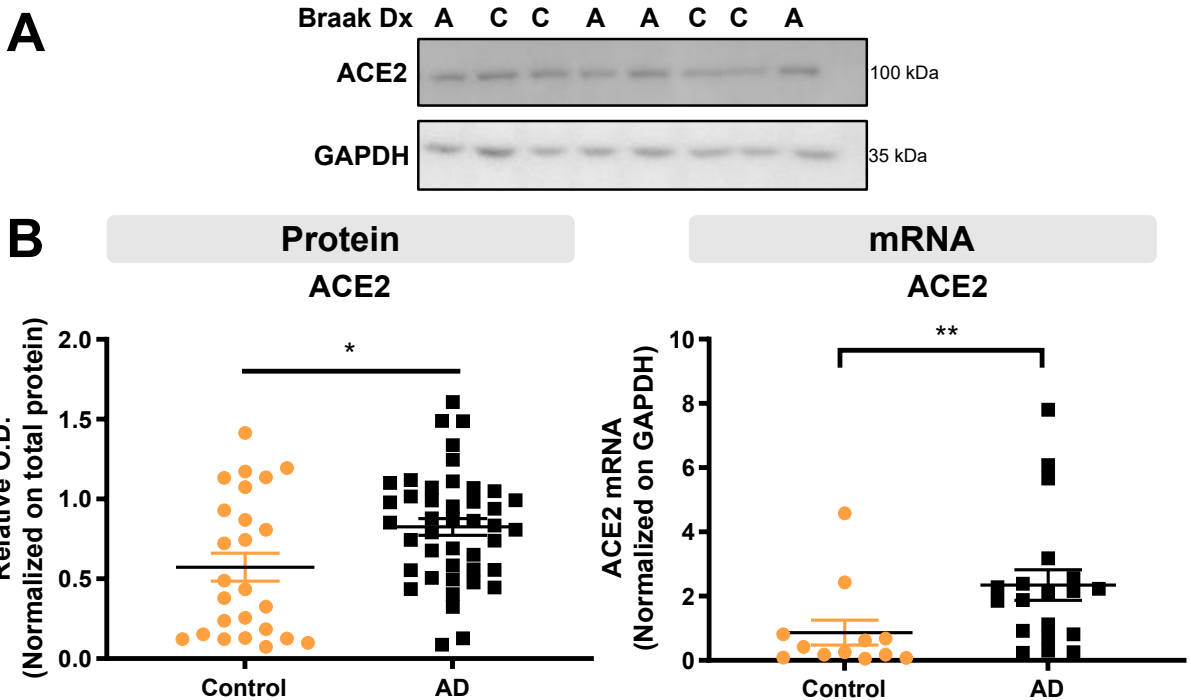

Figure 3

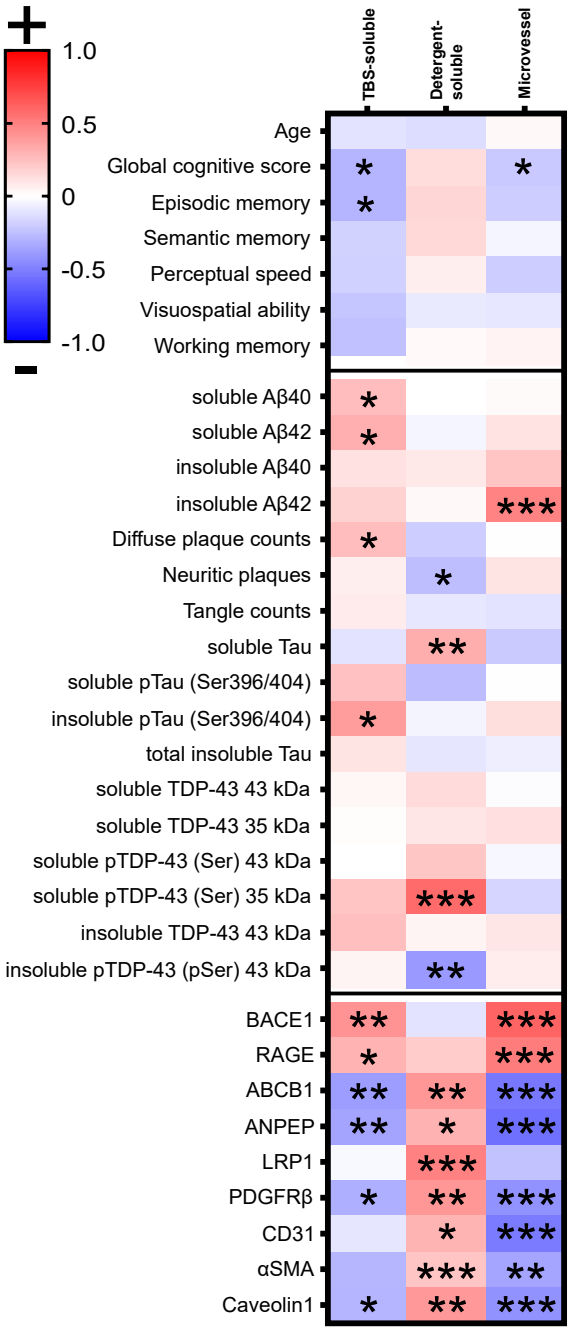
ACE2
TBS-soluble
Detergent-soluble
Microvessel
1.0
0.5
0
-0.5
-1.0
Age
Global cognitive score
Episodic memory
Semantic memory
Perceptual speed
Visuospatial ability
Working memory
antemortem evaluation
soluble Aβ40
soluble Aβ42
insoluble Aβ40
insoluble Aβ42
Diffuse plaque counts
Neuritic plaques
Tangle counts
soluble Tau
soluble pTau (Ser396/404)
insoluble pTau (Ser396/404)
total insoluble Tau
soluble TDP-43 43 kDa
soluble TDP-43 35 kDa
soluble pTDP-43 (Ser) 43 kDa
soluble pTDP-43 (Ser) 35 kDa
insoluble TDP-43 43 kDa
insoluble pTDP-43 (pSer) 43 kDa
neuropathological markers
BACE1
RAGE
ABCB1
ANPEP
LRP1
PDGFRβ
CD31
αSMA
Caveolin1
BBB markers

Figure 4

ACE2 in isolated microvessel-enriched fraction

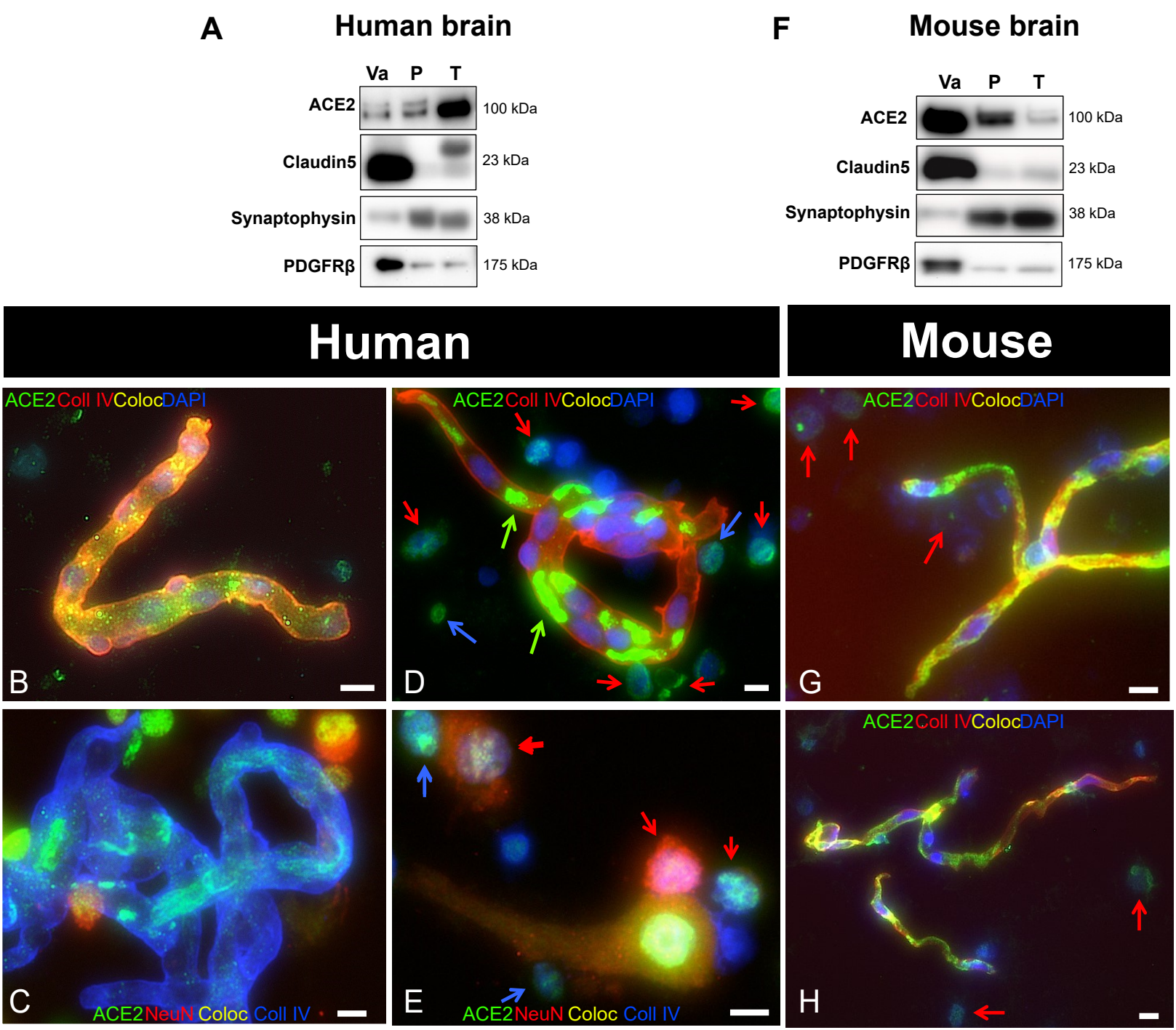

Figure 5

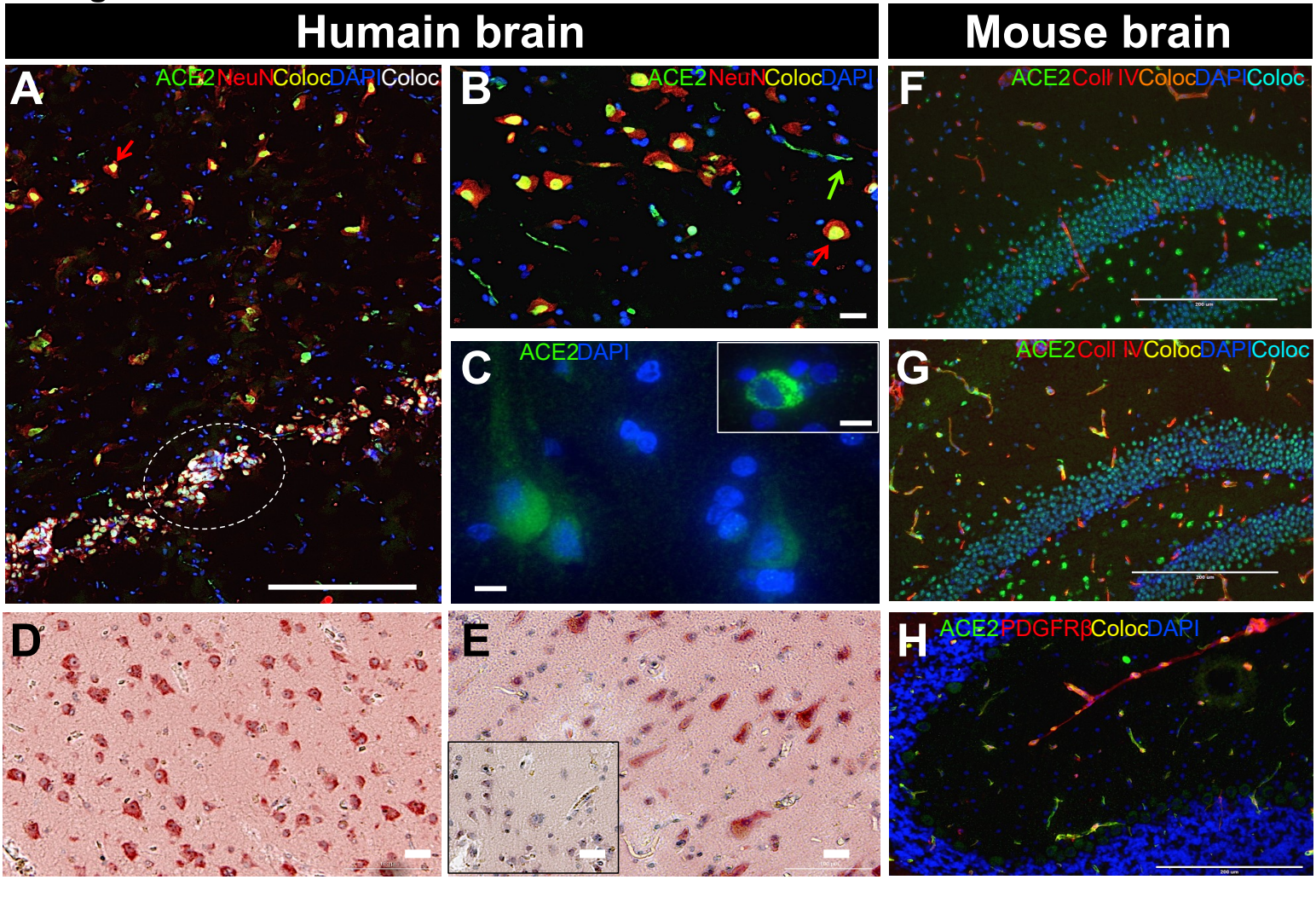
Humain brain
Mouse brain
A
ACE2NeuNColocDAPIColoc
B
ACE2NeuNColocDAPI
C
ACE2DAPI
D
E
F
ACE2Coll IVColocDAPIColoc
G
ACE2Coll IVColocDAPIColoc
H
ACE2PDGFRβColocDAPI

Figure 6

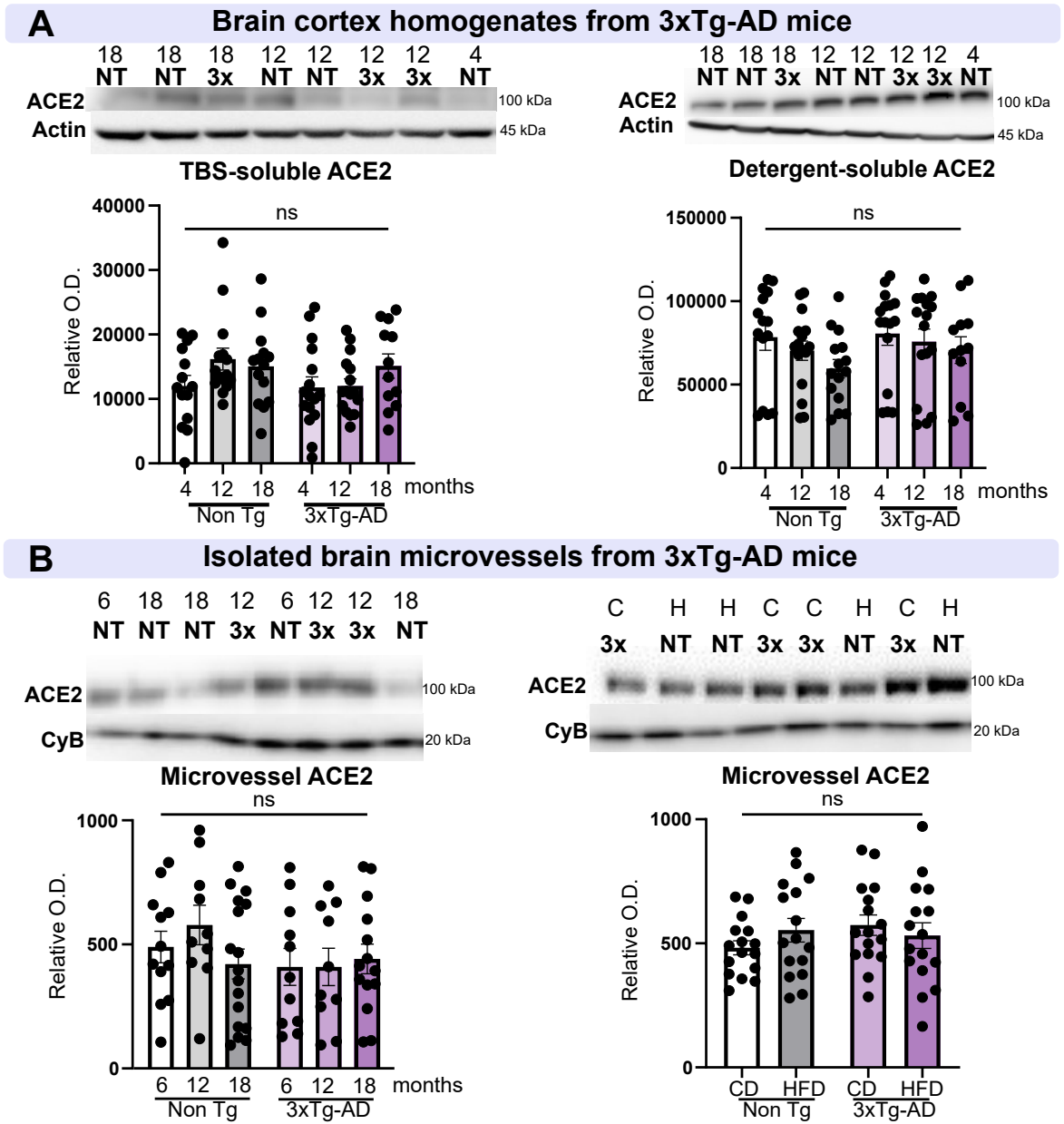
A
Brain cortex homogenates from 3xTg-AD mice
18 18 18 12 12 12 12 4
NT NT 3x NT NT 3x 3x NT
ACE2
Actin
100 kDa
45 kDa
TBS-soluble ACE2
Relative O.D.
ns
40000
30000
20000
10000
0
4 12 18 4 12 18 months
Non Tg
3xTg-AD
18 18 18 12 12 12 12 4
NT NT 3x NT NT 3x 3x NT
ACE2
Actin
100 kDa
45 kDa
Detergent-soluble ACE2
Relative O.D.
ns
150000
100000
50000
0
4 12 18 4 12 18 months
Non Tg
3xTg-AD
B
Isolated brain microvessels from 3xTg-AD mice
6 18 18 12 6 12 12 18
NT NT NT 3x NT 3x 3x NT
ACE2
CyB
100 kDa
20 kDa
Microvessel ACE2
Relative O.D.
ns
1000
500
0
6 12 18 6 12 18 months
Non Tg
3xTg-AD
C H H C C H C H
3x NT NT 3x 3x NT 3x NT
ACE2
CyB
100 kDa
20 kDa
Microvessel ACE2
Relative O.D.
ns
1000
500
0
CD HFD CD HFD
Non Tg
3xTg-AD

Religious Order Study (Cohort #1)			
Characteristics	**Control**	**AD**	**Statistical Analysis**
N	22	38	------
Men, %	41	29	C; Pearson test, $\chi^2 = 0.897$; p = 0.3436
Mean age at death	86.7 (4.3)	87.5 (5.7)	Mann Whitney test, p = 0.5548
post-mortem delay (h)	7.9 (5.1)	7.5 (5.1)	Mann Whitney test, p = 0.6648
Mean education, years	18.3 (3.5)	18.1 (3.1)	Mann Whitney test, p = 0.5236
Mean MMSE	25.0 (4.5)	21.6 (7.9)	Mann Whitney test, p = 0.0791
Global cognition score	-0.32 (0.8)	-0.94 (0.9)[#]	Mann Whitney test, p = 0.0044
apoE ε4 allele carriage (%)	9	45 $	C; Pearson test, $\chi^2 = 8.182$; p = 0.0042
Clinical diagnosis NCI/MCI/AD (n)	11/8/3	9/12/17	------
Thal amyloid score 0/1/2/3 (n)	7/13/2/0	0/3/15/20	------
Braak score 0/1/2/3 (n)	0/7/15/0	0/0/27/11	------
CERAD score 0/1/2/3 (n)	14/4/4/0	1/3/16/18	------
Parenchymal CAA stage in parietal cortex 0/1/2/3/4 (n)	15/4/1/1/0	18/7/5/2/3	C; Pearson test, $\chi^2 = 3.830$; p = 0.4295
Presence of chronic cortical macroinfarcts 0/1 (n)	20/2	33/5	C; Pearson test, $\chi^2 = 0.224$; p = 0.6363
Presence of chronic cortical microinfarcts 0/1 (n)	17/5	34/4	C; Pearson test, $\chi^2 = 1.627$; p = 0.2021
Usage of antihypertensive medications 0/1 (n)	2/20	5/33	C; Pearson test, $\chi^2 = 0.224$; p = 0.6363
Usage of diabetes medications 0/1 (n)	15/7	33/5	C; Pearson test, $\chi^2 = 3.032$; p = 0.0816
Cerebellar pH	6.4 (0.37)	6.3 (0.36)	Mann Whitney test, p = 0.2933
Diffuse Plaque Counts in parietal cortex	3.8 (8.0)	20.3 (16.8)[&]	Mann Whitney test, p < 0.0001
Neuritic Plaque Counts in parietal cortex	1.3 (3.2)	15.7 (12.5)[&]	Mann Whitney test, p < 0.0001
Neurofibrillary Tangle Counts	0.09 (0.43)	2.92 (8.35)[#]	Mann Whitney test, p = 0.0096
Soluble Aβ40 concentration, pmol/L	125.4 (245.9)	363.2 (695.2)[¶]	Mann Whitney test, p = 0.0009
Soluble Aβ42 concentration, pmol/L	299.6 (475.0)	1173.6 (503.9)[&]	Mann Whitney test, p < 0.0001
Soluble Aβ40/Aβ42 ratio	0.99 (1.09)	0.34 (0.59)	Mann Whitney test, p < 0.0001
Cyclophilin B in microvessel extracts (loading control)	2.74 (0.77)	2.66 (0.79)	Mann Whitney test, p = 0.7309
Claudin5 levels in microvessel extracts (normalized ROD)	1.17 (0.50)	1.16 (0.41)	Mann Whitney test, p = 0.6613
CD31 levels in microvessel extracts (normalized ROD)	0.45 (0.40)	0.41 (0.36)	Mann Whitney test, p = 0.7366
US other sources (Cohort #2)			
Characteristics	**Control**	**AD**	**Statistical Analysis**
N	30	52	------
Men, %	70	52	C; Pearson test, $\chi^2 = 2.561$; p = 0.1095
Mean age at death	74.9 (9.7)	78.9 (14.0)	Unpaired t test, p = 0.0784
post-mortem delay (h)	16.3 (4.9)	17.6 (4.8)	Unpaired t test, p = 0.2185
Braak stages 0-2/3-6 (n)	30/0	0/52	------
Atherosclerosis (%)	n.d.	61,5	------

Figure S1

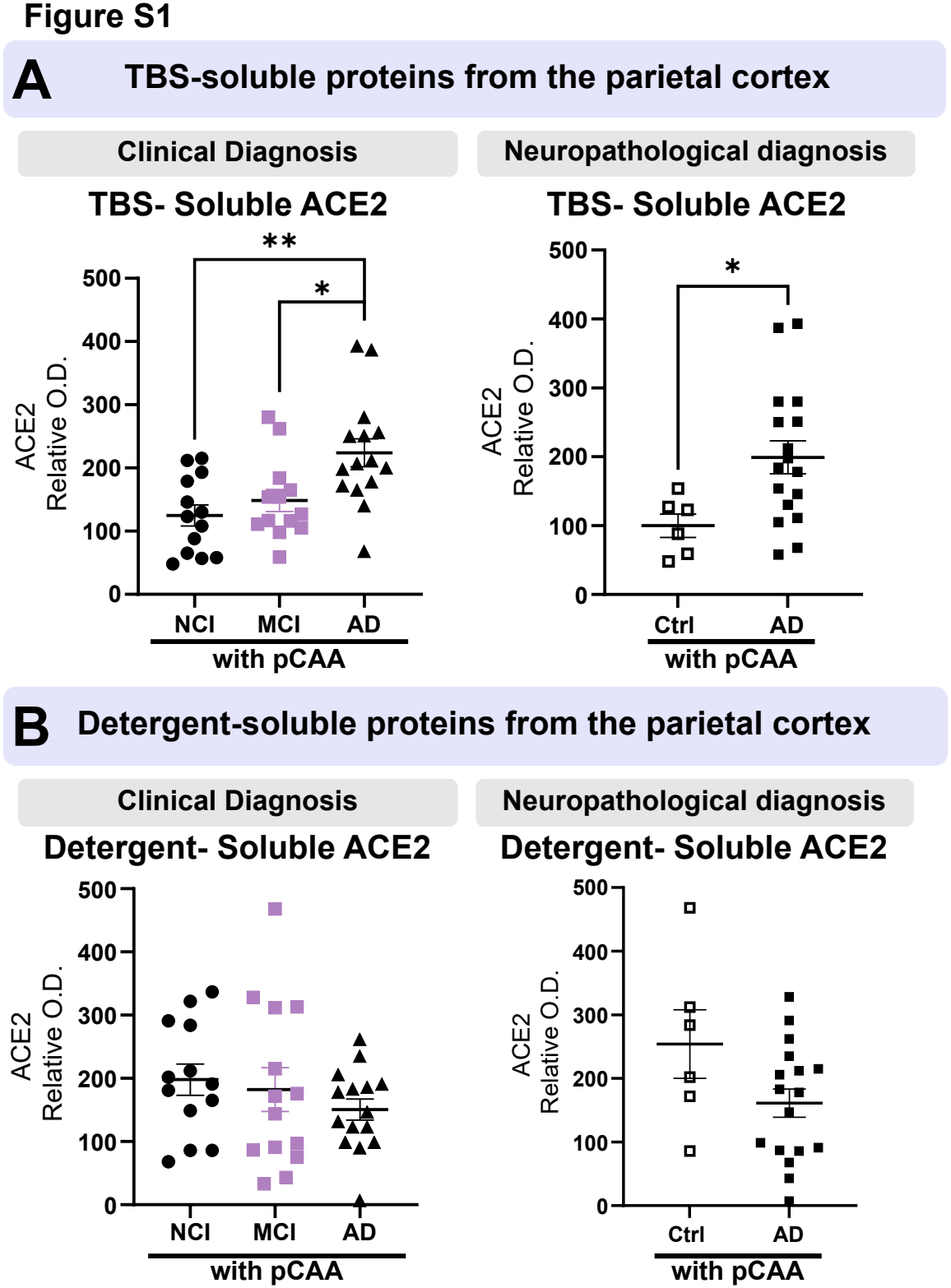
A
TBS-soluble proteins from the parietal cortex
Clinical Diagnosis
Neuropathological diagnosis
TBS- Soluble ACE2
TBS- Soluble ACE2
**
*
*
ACE2
Relative O.D.
500
400
300
200
100
0
NCI
MCI
AD
Ctrl
AD
with pCAA
with pCAA
B
Detergent-soluble proteins from the parietal cortex
Clinical Diagnosis
Neuropathological diagnosis
Detergent- Soluble ACE2
Detergent- Soluble ACE2
ACE2
Relative O.D.
500
400
300
200
100
0
NCI
MCI
AD
Ctrl
AD
with pCAA
with pCAA

Figure S2

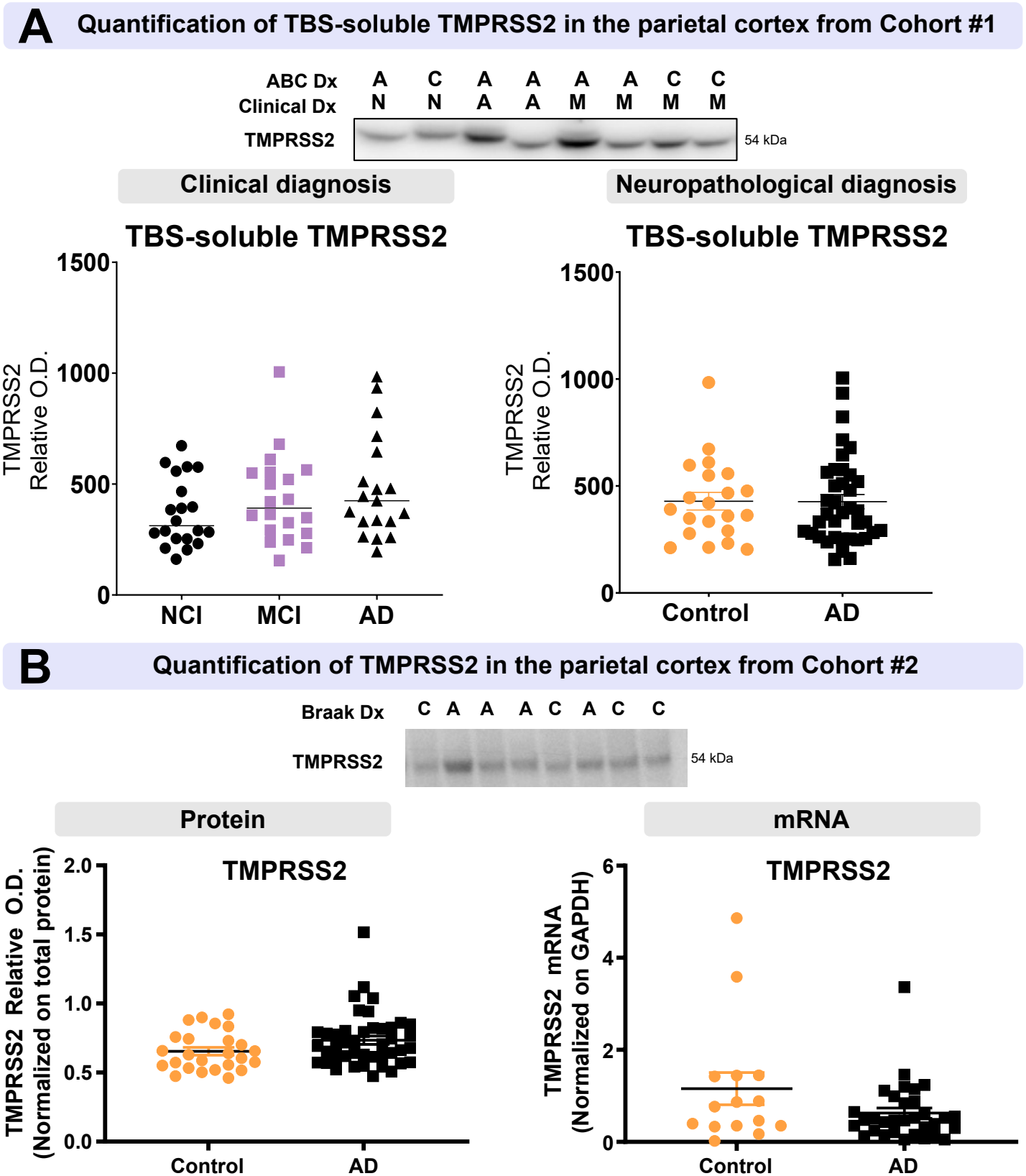
A
Quantification of TBS-soluble TMPRSS2 in the parietal cortex from Cohort #1
ABC Dx
Clinical Dx
A N
C N
A A
A A
A M
A M
C M
C M
TMPRSS2
54 kDa
Clinical diagnosis
Neuropathological diagnosis
TBS-soluble TMPRSS2
TMPRSS2 Relative O.D.
1500
1000
500
0
NCI
MCI
AD
Control
AD
B
Quantification of TMPRSS2 in the parietal cortex from Cohort #2
Braak Dx
C A A A C A C C
TMPRSS2
54 kDa
Protein
mRNA
TMPRSS2
TMPRSS2 Relative O.D. (Normalized on total protein)
2.0
1.5
1.0
0.5
0.0
TMPRSS2 mRNA (Normalized on GAPDH)
6
4
2
0
Control
AD

Figure S3

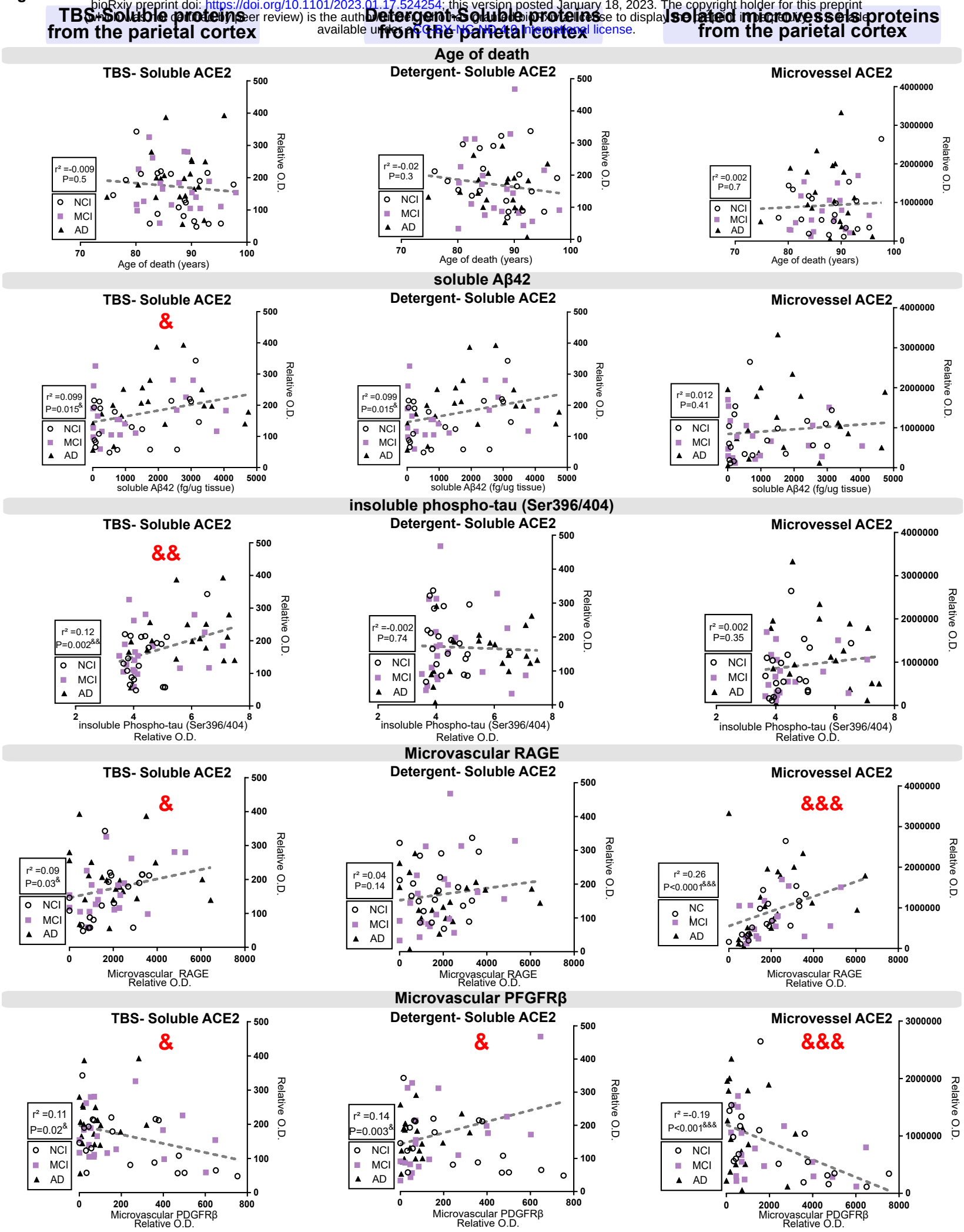

Figure S4

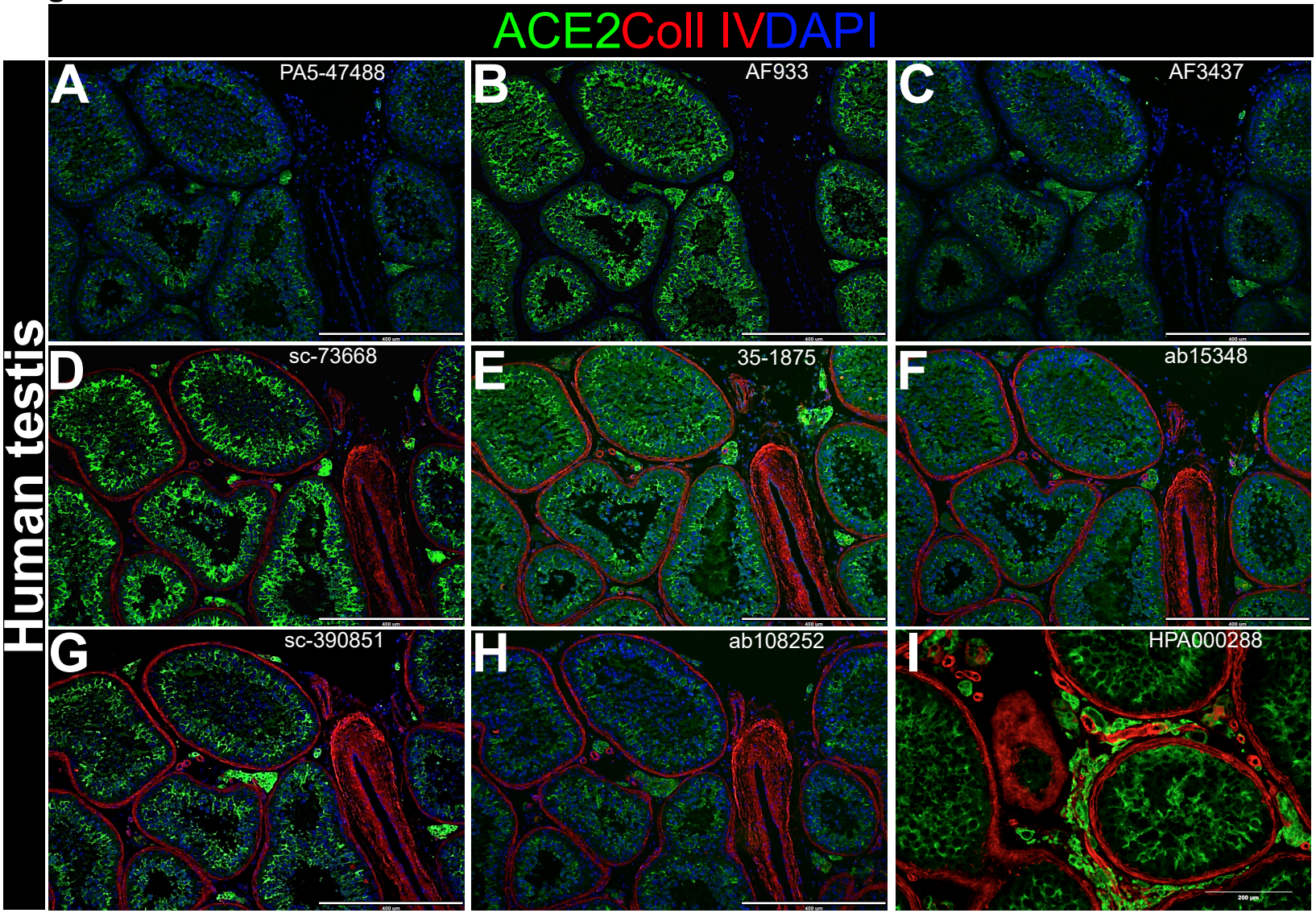
ACE2ColI IVDAPI
Human testis
A
PA5-47488
B
AF933
C
AF3437
D
sc-73668
E
35-1875
F
ab15348
G
sc-390851
H
ab108252
I
HPA000288

Figure S5 **Measurements in human parietal cortex from Cohort#1**

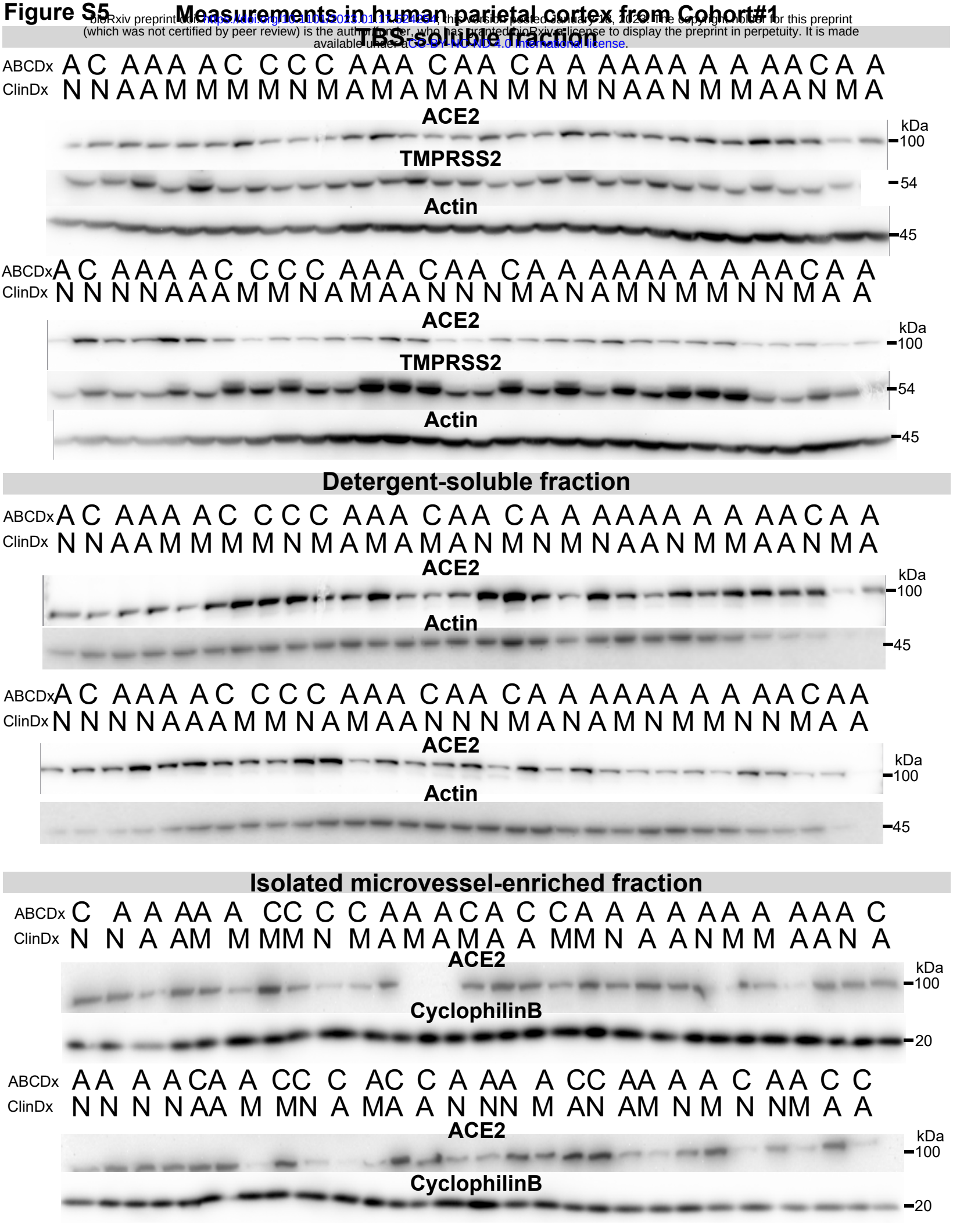

Figure S6 **Measurements in human parietal cortex from Cohort#2**

Brain homogenates from parietal cortex